



Markus Lazar

# Incompatible strain gradient elasticity of Mindlin type: screw and edge dislocations

Received: 15 February 2021 / Accepted: 22 April 2021  
© The Author(s) 2021

**Abstract** The fundamental problem of dislocations in incompatible isotropic strain gradient elasticity theory of Mindlin type, unsolved for more than half a century, is solved in this work. Incompatible strain gradient elasticity of Mindlin type is the generalization of Mindlin's compatible strain gradient elasticity including plastic fields providing in this way a proper eigenstrain framework for the study of defects like dislocations. Exact analytical solutions for the displacement fields, elastic distortions, Cauchy stresses, plastic distortions and dislocation densities of screw and edge dislocations are derived. For the numerical analysis of the dislocation fields, elastic constants and gradient elastic constants have been used taken from ab initio DFT calculations. The displacement, elastic distortion, plastic distortion and Cauchy stress fields of screw and edge dislocations are non-singular, finite, and smooth. The dislocation fields of a screw dislocation depend on one characteristic length, whereas the dislocation fields of an edge dislocation depend on up to three characteristic lengths. For a screw dislocation, the dislocation fields obtained in incompatible strain gradient elasticity of Mindlin type agree with the corresponding ones in simplified incompatible strain gradient elasticity. In the case of an edge dislocation, the dislocation fields obtained in incompatible strain gradient elasticity of Mindlin type are depicted more realistic than the corresponding ones in simplified incompatible strain gradient elasticity. Among others, the Cauchy stress of an edge dislocation obtained in incompatible isotropic strain gradient elasticity of Mindlin type looks more physical in the dislocation core region than the Cauchy stress obtained in simplified incompatible strain gradient elasticity and is in good agreement with the stress fields of an edge dislocation computed in atomistic simulations. Moreover, it is shown that the shape of the dislocation core of an edge dislocation has a more realistic asymmetric form due to its inherent asymmetry in incompatible isotropic strain gradient elasticity of Mindlin type than the dislocation core possessing a cylindrical symmetry in simplified incompatible strain gradient elasticity. It is revealed that the considered theory with the incorporation of three characteristic lengths offers a more realistic description of an edge dislocation than the simplified incompatible strain gradient elasticity with only one characteristic length.

## 1 Introduction

A dislocation is the elementary carrier of plasticity in crystals and the most important crystal defect. Therefore, plasticity is based on dislocations, in particular on the glide of dislocations. The natural scale of the mechanics of dislocations is the Ångström scale, which is the characteristic scale in crystallography. However, all fields of dislocations using classical dislocation theory possess singularities, like the  $1/r$ -type singularity in the stress and elastic strain fields of dislocations, because the classical approach is not valid at small scales like the Ångström scale (see, e.g., [6, 12, 17, 41]).

---

M. Lazar (✉)  
Karlsruhe Institute of Technology (KIT), Institute of Engineering Mechanics, 76131 Karlsruhe, Germany  
E-mail: markus.lazar@kit.edu

Generalized continuum theories, like gradient elasticity and nonlocal elasticity, are continuum theories valid at small scales (see, e.g., [7,27,30]). Mindlin [32] (see also [33]) derived the theory of compatible first strain gradient elasticity. Compatible first strain gradient elasticity incorporates the gradient of the elastic strain tensor in the elastic energy in addition to the elastic strain tensor. For an isotropic material, this framework is characterized by the two Lamé constants and five strain gradient parameters leading to two characteristic lengths. Mindlin's first strain gradient elasticity theory respects the invariance under the group  $SO(3)$  and their irreducible representations (see [26]). Already, Toupin and Grazis [47] and Mindlin [34] (see also [13]) pointed out that first strain gradient elasticity, sometimes called gradient elasticity of grade-2, can be considered as the continuum version of a lattice theory with up to second-neighbor interactions (nearest and next-nearest neighbor interactions). Using ab initio density functional theory (DFT) calculations, Shodja et al. [45] showed that the characteristic lengths of Mindlin's compatible strain gradient elasticity theory are in the order of  $\sim 10^{-10}$  m (Ångström) for several fcc and bcc materials. The elements of the Hessian matrix, obtained by taking the second derivatives of the total energy with respect to the atomic positions, are related to the strain gradient material constants. Nowadays, the material parameters of first strain gradient elasticity can be computed from interatomic potentials to be a self-consistent and parameter-free field theory of materials [1,40]. Moreover, the atomistic representation of the constitutive tensors in first strain gradient elasticity was given by Admal et al. [1]. The atomistic representations are analytical expressions in terms of the first and second derivatives of the interatomic potential with respect to interatomic distances, and dyadic products of relative atomic positions (see [1]).

First efforts toward dislocations in the framework of Mindlin's strain gradient elasticity were carried out by Lardner [16] and Rogula [42], who considered screw and edge dislocations in the framework of Mindlin's compatible strain gradient elasticity [32]. Considering neither plastic distortion nor dislocation density, Lardner [16] and Rogula [42] constructed solutions to a compatible elastic boundary value problem and consequently failed to remove the classical singularities.

More than two decades later, using a simplified theory of gradient elasticity with only one characteristic length scale parameter, non-singular elastic strain fields of screw and edge dislocations were given, for the first time, by Gutkin and Aifantis [8,9]. Non-singular stress and strain fields of screw and edge dislocations based on a simplified gradient elasticity (or gradient elasticity of Helmholtz type) were given by Lazar and Maugin [18] (see also [19]). Simplified strain gradient elasticity is a particular version of Mindlin's strain gradient elasticity where the double stress tensor can be expressed in a particular form in terms of the gradient of the Cauchy stress tensor (see, e.g., [18,26]). Moreover, Lazar and Maugin [20] have shown for straight dislocations that the gradient terms with the characteristic length scale parameter lead to a smoothing of the displacement profile, in contrast with the jump occurring in the classical displacement field. Simplified incompatible gradient elasticity (gradient elasticity of Helmholtz type) provides robust non-singular solutions including one length scale parameter for the elastic distortion, plastic distortion, stress and displacement fields of screw and edge dislocations. An important mathematical property of gradient elasticity is that it provides a regularization based on partial differential equations (PDEs) of higher order where the characteristic length scale parameter plays the role of a regularization parameter. Afterward, the non-singular expressions of all dislocation key equations were given by Lazar [23–25] for dislocation loops using simplified gradient elasticity. For dislocations, the incompatible version of simplified gradient elasticity including plastic distortion and dislocation density tensors is used leading to an incompatible strain gradient elasticity of defects. These non-singular dislocation key equations (Burgers formula, Mura–Willis equation, and Peach–Koehler stress formula) have been implemented in the UCLA Discrete Dislocation Dynamics (DD) code called “model” [35] and used for applications [39]. The results of the dislocation fields in simplified gradient elasticity endow DD with a level of maturity that is necessary for computer simulations of three-dimensional dislocation ensembles with near atomic resolution. Therefore, the use of strain gradient elasticity theory for micromechanical problems of dislocations leads to non-singular and smooth dislocation fields, and in this way to an Ångström-mechanics of dislocations (see also [30]). Nevertheless, for a more realistic and physically based modeling of an edge dislocation due to its inherent asymmetry more than one characteristic length scale parameter is necessary, and this is exactly what Mindlin's strain gradient elasticity offers.

Using an incompatible version of Mindlin's strain gradient elasticity and the technique of Fourier transform, non-singular and smooth displacement fields of screw and edge dislocations have been recently reported by Delfani and Tavakol [3] and Delfani et al. [4], respectively. Delfani and Tavakol [3] and Delfani et al. [4] have reproduced the smoothing of the displacement profile of screw and edge dislocations. However, a systematic and complete study of screw and edge dislocations (including the elastic strain and stress fields) in the incompatible

framework of Mindlin's strain gradient elasticity is still missing in the literature. Therefore, the present work aims to close this gap in the literature of dislocations in strain gradient elasticity.

The purpose of the present work is to find solutions for the displacement, plastic distortion, dislocation density, stress and elastic distortion fields of screw and edge dislocations within the framework of incompatible isotropic strain gradient elasticity theory of Mindlin type. This is an unsolved fundamental problem for more than half a century. We will formulate the eigenstrain problem of dislocations in Mindlin's isotropic gradient elasticity. Dislocation problems are typical examples of eigenstrain problems (see, e.g., [31,36]). We will use the two-dimensional Green tensors (fundamental solutions of the Mindlin operator) to find non-singular dislocation fields for a given eigenstrain (or plastic distortion). Furthermore, we clarify the question of the influence on the dislocation solutions of different characteristic length scale parameters and the five gradient parameters of the incompatible isotropic strain gradient elasticity theory of Mindlin type and the similarities and differences to the dislocation solutions obtained in the framework of simplified incompatible strain gradient elasticity. For the numerical computations, the values of the five gradient parameters for aluminum will be used given by Shodja [45,46] using atomistic ab initio DFT calculations.

The paper is organized as follows. In Sect. 2, we give the basics of incompatible strain gradient elasticity of Mindlin type including the relevant Green's functions which are necessary to solve the field equations for prescribed plastic distortion of a dislocation. Using the technique of Green's functions and convolution, solutions of screw and edge dislocations are presented in Sects. 3 and 4, respectively. The limit of the solutions of screw and edge dislocations in incompatible strain gradient elasticity of Mindlin type toward simplified incompatible gradient elasticity is given in Sect. 5. In Sect. 6, conclusions are given. Some technical details are reported in the "Appendix."

## 2 Incompatible strain gradient elasticity of Mindlin type

In this Section, we present the structure and framework of the theory of incompatible strain gradient elasticity of Mindlin type, which is the incompatible generalization of Mindlin's compatible first strain gradient elasticity and is suitable as defect theory at small scales down to the Ångström scale.

### 2.1 General form

Consider an infinite elastic body. In Mindlin's theory of first strain gradient elasticity [32,33], the strain energy density for centrosymmetric materials reads as

$$\mathcal{W}(\mathbf{e}, \nabla \mathbf{e}) = \frac{1}{2} \mathbb{C}_{ijkl} e_{ij} e_{kl} + \frac{1}{2} \mathbb{D}_{ijmkl} \partial_m e_{ij} \partial_n e_{kl}. \quad (1)$$

Here  $e_{ij}$  denotes the incompatible elastic strain tensor which is given by

$$e_{ij} = \frac{1}{2} (\beta_{ij} + \beta_{ji}) \quad (2)$$

and is nothing but the symmetric part of the incompatible elastic distortion tensor

$$\beta_{ij} = \partial_j u_i - \beta_{ij}^P, \quad (3)$$

which is given in terms of the gradient of the displacement vector  $u_i$  and the plastic distortion (or eigendistortion) tensor  $\beta_{ij}^P$ .

Moreover,  $\mathbb{C}_{ijkl}$  is the fourth-rank matter tensor (constitutive tensor) of the elastic constants possessing the minor symmetries

$$\mathbb{C}_{ijkl} = \mathbb{C}_{jikl} = \mathbb{C}_{ijlk} \quad (4)$$

and the major symmetry

$$\mathbb{C}_{ijkl} = \mathbb{C}_{klij}, \quad (5)$$

whereas  $\mathbb{D}_{ijmkl n}$  is the sixth-rank matter tensor (constitutive tensor) of the gradient elastic constants possessing the minor symmetries

$$\mathbb{D}_{ijmkl n} = \mathbb{D}_{jimkl n} = \mathbb{D}_{ijmkl n} \quad (6)$$

and the major symmetry

$$\mathbb{D}_{ijmkl n} = \mathbb{D}_{klnijm} . \quad (7)$$

The quantities conjugate to the elastic strain tensor  $e_{ij}$  and the gradient of the elastic strain tensor  $\partial_m e_{ij}$  are the Cauchy stress tensor  $\sigma_{ij}$  and the double stress tensor  $\tau_{ijm}$ , respectively. They are defined as

$$\sigma_{ij} = \frac{\partial \mathcal{W}}{\partial e_{ij}} = \mathbb{C}_{ijkl} e_{kl} , \quad (8)$$

$$\tau_{ijm} = \frac{\partial \mathcal{W}}{\partial (\partial_m e_{ij})} = \mathbb{D}_{ijmkl n} \partial_n e_{kl} . \quad (9)$$

In dislocation theory, the dislocation density tensor is defined in terms of the incompatible plastic distortion tensor (see, e.g., [15,25])

$$\alpha_{ij} = -\epsilon_{jkl} \partial_k \beta_{il}^P , \quad (10)$$

and in terms of the incompatible elastic distortion tensor

$$\alpha_{ij} = \epsilon_{jkl} \partial_k \beta_{il} , \quad (11)$$

where  $\epsilon_{jkl}$  denotes the Levi-Civita tensor. In other words, the dislocation density tensor is the incompatibility tensor due to dislocations, and it gives the characteristic shape and size of the dislocation core. The dislocation density tensor satisfies the Bianchi identity of dislocations,

$$\partial_j \alpha_{ij} = 0 , \quad (12)$$

which means that dislocations cannot end inside the body.

The condition of static equilibrium is expressed by the Euler–Lagrange equation, and it reads in first strain gradient elasticity

$$\frac{\delta \mathcal{W}}{\delta u_i} = \frac{\partial \mathcal{W}}{\partial u_i} - \partial_j \frac{\partial \mathcal{W}}{\partial (\partial_j u_i)} + \partial_k \partial_j \frac{\partial \mathcal{W}}{\partial (\partial_k \partial_j u_i)} = 0 . \quad (13)$$

In terms of the Cauchy stress and double stress tensors, Eq. (13) takes the form [32]

$$\partial_j (\sigma_{ij} - \partial_k \tau_{ijk}) = 0 . \quad (14)$$

Because dislocations cause self-stresses, no physical body forces are present in the equilibrium condition for dislocations. Dislocations belong to the category of eigenstrain problems (see [6,36]).

## 2.2 Isotropic form

Consider now the isotropic version of Mindlin’s strain gradient elasticity theory of form II. Using  $SO(3)$ -invariance arguments, an isotropic matter tensor of rank 4, satisfying Eqs. (4) and (5), reads as

$$\mathbb{C}_{ijkl} = \lambda \delta_{ij} \delta_{kl} + \mu (\delta_{ik} \delta_{jl} + \delta_{il} \delta_{jk}) , \quad (15)$$

where  $\lambda$  and  $\mu$  are the Lamé constants (elastic constants) and  $\delta_{ij}$  is the Kronecker symbol, and an isotropic matter tensor of rank 6, satisfying Eqs. (6) and (7), reads as

$$\begin{aligned} \mathbb{D}_{ijmkl n} = & \frac{a_1}{2} (\delta_{ij} \delta_{km} \delta_{ln} + \delta_{ij} \delta_{kn} \delta_{lm} + \delta_{kl} \delta_{im} \delta_{jn} + \delta_{kl} \delta_{in} \delta_{jm}) + 2a_2 \delta_{ij} \delta_{kl} \delta_{mn} \\ & + \frac{a_3}{2} (\delta_{jk} \delta_{im} \delta_{ln} + \delta_{ik} \delta_{jm} \delta_{ln} + \delta_{il} \delta_{jm} \delta_{kn} + \delta_{jl} \delta_{im} \delta_{kn}) + a_4 (\delta_{il} \delta_{jk} \delta_{mn} + \delta_{ik} \delta_{jl} \delta_{mn}) \end{aligned}$$

$$+ \frac{a_5}{2} (\delta_{jk} \delta_{in} \delta_{lm} + \delta_{ik} \delta_{jn} \delta_{lm} + \delta_{jl} \delta_{km} \delta_{in} + \delta_{il} \delta_{km} \delta_{jn}), \quad (16)$$

where  $a_1, a_2, a_3, a_4, a_5$  are the five strain gradient parameters (or gradient elastic constants) in Mindlin's isotropic first strain gradient elasticity theory [32] (see also [26,33]).

For the isotropic case, the Cauchy stress tensor is given by

$$\sigma_{ij} = 2\mu e_{ij} + \lambda \delta_{ij} e_{ll}, \quad (17)$$

and the double stress tensor is given by

$$\begin{aligned} \tau_{ijk} = & \frac{a_1}{2} (\delta_{ik} \partial_j e_{ll} + \delta_{jk} \partial_i e_{ll} + 2\delta_{ij} \partial_l e_{kl}) + 2a_2 \delta_{ij} \partial_k e_{ll} \\ & + a_3 (\delta_{ik} \partial_l e_{jl} + \delta_{jk} \partial_l e_{il}) + 2a_4 \partial_k e_{ij} + a_5 (\partial_i e_{jk} + \partial_j e_{ki}). \end{aligned} \quad (18)$$

Using Eqs. (2), (8), and (9), Eq. (14) can be cast in the following equation in terms of the displacement vector and the plastic distortion tensor:

$$L_{ik}^M u_k = \mu [1 - \ell_2^2 \Delta] (\partial_l \beta_{il}^P + \partial_l \beta_{li}^P) + [\lambda - (a_1 + 2a_2) \Delta] \partial_i \beta_{ll}^P - (a_1 + a_3 + a_5) \partial_i \partial_k \partial_l \beta_{kl}^P, \quad (19)$$

where  $L_{ik}^M$  denotes the tensorial linear partial differential operator arising in Mindlin's first strain gradient elasticity called the Mindlin operator. The isotropic Mindlin operator (differential operator of fourth order) is given by

$$L_{ik}^M = (\lambda + 2\mu) [1 - \ell_1^2 \Delta] \partial_i \partial_k + \mu [1 - \ell_2^2 \Delta] (\delta_{ik} \Delta - \partial_i \partial_k), \quad (20)$$

where  $\Delta$  indicates the Laplace operator (differential operator of second order) and the two characteristic lengths, defined in terms of the five gradient elastic constants and the two elastic constants (Lamé constants), which are known in isotropic compatible strain gradient elasticity of Mindlin type,

$$\ell_1^2 = \frac{2(a_1 + a_2 + a_3 + a_4 + a_5)}{\lambda + 2\mu}, \quad (21)$$

$$\ell_2^2 = \frac{a_3 + 2a_4 + a_5}{2\mu}. \quad (22)$$

The two characteristic lengths  $\ell_1$  and  $\ell_2$  are the length scales appearing in the isotropic Mindlin operator (20), and they are the characteristic length scales for the displacement vector  $u_k$ . Therefore, the two characteristic lengths  $\ell_1$  and  $\ell_2$  are the length scales appearing in Mindlin's isotropic compatible gradient elasticity (see [28,32]). Also, it can be observed on the right-hand side of Eq. (19) that the gradient elastic constants  $a_1, a_3,$  and  $a_5$  play a particular role for the plastic distortion.

Now, we decompose the plastic distortion tensor  $\beta_{ij}^P$  into its deviatoric (traceless) part  $\hat{\beta}_{ij}^P$ , which we call deviatoric plastic distortion tensor, and its trace  $\beta_{ll}^P$ , which is the plastic dilatation:

$$\beta_{ij}^P = \hat{\beta}_{ij}^P + \frac{1}{3} \delta_{ij} \beta_{ll}^P \quad (23)$$

with  $\hat{\beta}_{ll}^P = 0$ . If we substitute the decomposition (23) into Eq. (19), the mathematical structure of the right-hand side of Eq. (19) becomes more visible,

$$L_{ik}^M u_k = \mu L_2 (\partial_l \hat{\beta}_{il}^P + \partial_l \hat{\beta}_{li}^P) + \frac{1}{3} (2\mu + 3\lambda) L_3 \partial_i \beta_{ll}^P + 2\mu (\ell_2^2 - \ell_4^2) \partial_i \partial_k \partial_l \hat{\beta}_{kl}^P, \quad (24)$$

where the isotropic scalar Helmholtz operator (differential operator of second order) is defined by

$$L_j = 1 - \ell_j^2 \Delta, \quad \ell_j > 0. \quad (25)$$

Here,  $\ell_j$  are positive real length scale parameters. Sometimes, the differential operator (25) is called modified Helmholtz operator [49] or metaharmonic operator [37]. In Eq. (24), it becomes obvious that in isotropic

incompatible strain gradient elasticity of Mindlin type, two additional characteristic lengths can be defined in terms of the five gradient elastic constants and the two elastic constants (Lamé constants), namely

$$\ell_3^2 = \frac{2(2a_1 + 3a_2 + a_3 + a_4 + a_5)}{3\lambda + 2\mu}, \quad (26)$$

$$\ell_4^2 = \frac{a_1 + 2a_3 + 2a_4 + 2a_5}{2\mu}. \quad (27)$$

The two characteristic lengths  $\ell_3$  and  $\ell_4$  are additional length scales due to the plastic distortion tensor appearing on the right-hand side of Eq. (24). The length scale  $\ell_3$  is the characteristic length of the plastic dilatation. On the other hand, the divergence of Eq. (24) gives

$$(2\mu + \lambda)L_1 \Delta \partial_k u_k = \frac{1}{3}(2\mu + 3\lambda)L_3 \Delta \beta_{il}^P + 2\mu L_4 \partial_k \partial_l \beta_{kl}^P. \quad (28)$$

Moreover, Eq. (24) can be cast in the following form:

$$L_{ik}^M u_k + f_i = 0 \quad (29)$$

with the fictitious body force due to the plastic distortion

$$f_i = -\left[ \mu L_2 (\partial_l \beta_{il}^P + \partial_l \beta_{li}^P) + \frac{1}{3} (2\mu + 3\lambda) L_3 \partial_i \beta_{il}^P + 2\mu (\ell_2^2 - \ell_4^2) \partial_i \partial_k \partial_l \beta_{kl}^P \right]. \quad (30)$$

The difficulty in the theory of incompatible strain gradient elasticity of Mindlin type is that both fields, the displacement field  $u_k$  on the left-hand side and the plastic distortion  $\beta_{il}^P$  on the right-hand side of Eq. (19), are ‘‘a priori’’ unknown, and an operator decomposition of the Mindlin operator (20) might be helpful, which is given in the next Section.

### 2.3 Decomposition of the isotropic Mindlin operator

The operator decomposition used in incompatible strain gradient elasticity of Helmholtz type [25] or in simplified strain gradient elasticity [43] is based on the decomposition of a partial differential equation (PDE) of higher order into a system of PDEs of lower order and on the property that the appearing differential operator can be decomposed into a product of differential operators of lower order. Here, we present such an operator decomposition valid in incompatible strain gradient elasticity of Mindlin type.

Because the Mindlin operator (20) is a decomposable linear partial differential operator, it can be decomposed into an inner product of two tensorial linear partial differential operators,

$$L_{ik}^M = L_{il}^{(0)} L_{lk}^H = L_{il}^H L_{lk}^{(0)}, \quad (31)$$

where  $L_{il}^{(0)}$  is the isotropic Navier operator (differential operator of second order)

$$L_{ik}^{(0)} = (\lambda + 2\mu) \partial_i \partial_k + \mu (\delta_{ik} \Delta - \partial_i \partial_k) \quad (32)$$

and  $L_{lk}^H$  is a tensorial Helmholtz type operator (differential operator of second order) given by

$$L_{lk}^H = \delta_{lk} - \ell_1^2 \partial_l \partial_k - \ell_2^2 (\delta_{lk} \Delta - \partial_l \partial_k), \quad (33)$$

which is the tensorial generalization of the scalar Helmholtz operator  $L = 1 - \ell^2 \Delta$ . In the case that  $\ell_1 = \ell_2 = \ell$ , it reduces to:  $L_{lk}^H = \delta_{lk} (1 - \ell^2 \Delta) = \delta_{lk} L$ .

Using the operator decomposition (31), the inhomogeneous PDE (29) of fourth order

$$L_{il}^{(0)} L_{lk}^H u_k + f_i = 0 \quad (34)$$

might be decomposed into a system of PDEs of second order, namely the inhomogeneous tensorial Helmholtz type equation,

$$L_{lk}^H u_k = u_l^{(0)}, \quad (35)$$

and the classical inhomogeneous Navier equation of incompatible elasticity or eigenstrain theory,

$$L_{il}^{(0)} u_i^{(0)} + f_i = 0, \quad (36)$$

where  $u_i^{(0)}$  is the classical displacement field and  $f_i$  is the fictitious body force due to the classical plastic distortion  $\beta_{il}^{P,0}$  (see also [5])

$$\begin{aligned} f_i &= -[\mu(\partial_l \beta_{il}^{P,0} + \partial_l \beta_{li}^{P,0}) + \lambda \partial_i \beta_{ll}^{P,0}] \\ &= -[\mu(\partial_l \hat{\beta}_{il}^{P,0} + \partial_l \hat{\beta}_{li}^{P,0}) + \frac{1}{3}(2\mu + 3\lambda)\partial_i \beta_{ll}^{P,0}]. \end{aligned} \quad (37)$$

Thus, Eq. (37) represents the body force equivalent for dislocations in the framework of eigenstrain.

By combining Eqs. (30) and (37), the following PDE results for the plastic distortion tensor<sup>1</sup>:

$$\begin{aligned} \mu L_2(\partial_l \hat{\beta}_{il}^P + \partial_l \hat{\beta}_{li}^P) + \frac{1}{3}(2\mu + 3\lambda)L_3 \partial_i \beta_{ll}^P + 2\mu(\ell_2^2 - \ell_4^2)\partial_i \partial_k \partial_l \hat{\beta}_{kl}^P \\ = \mu(\partial_l \hat{\beta}_{il}^{P,0} + \partial_l \hat{\beta}_{li}^{P,0}) + \frac{1}{3}(2\mu + 3\lambda)\partial_i \beta_{ll}^{P,0}. \end{aligned} \quad (38)$$

If the deviatoric plastic distortion is zero, then Eq. (38) simplifies for the plastic dilatation  $\beta_{ll}^P$  to an inhomogeneous Helmholtz equation with characteristic length scale  $\ell_3$ :

$$L_3 \beta_{ll}^P = \beta_{ll}^{P,0}. \quad (39)$$

For instance, the length scale  $\ell_3$  is important for the plastic dilatation of a dilatation point defect (see, e.g., [29]). Substituting Eq. (38) into Eq. (24), we obtain the fundamental equation where the displacement vector  $u_k$  is determined by the classical plastic distortion tensor, which acts as prescribed plastic distortion,

$$L_{ik}^M u_k = \mu(\partial_l \beta_{il}^{P,0} + \partial_l \beta_{li}^{P,0}) + \lambda \partial_i \beta_{ll}^{P,0}. \quad (40)$$

The important consequence of the operator decomposition is that the displacement field  $u_k$  and the plastic distortion  $\beta_{ij}^P$  are obtained by the prescribed classical plastic distortion by solving the PDEs (40) and (38), respectively.

## 2.4 Green tensors of linear partial differential operators in incompatible strain gradient elasticity

In this Section, we present the Green tensors which arise from the dislocation problem in incompatible strain gradient elasticity of Mindlin type.

### 2.4.1 Green tensor of the isotropic Mindlin operator

First, we give the Green tensor of the Mindlin operator (20) for the case of an infinite isotropic medium needed for the solutions of the screw and edge dislocation problems. The Green tensor, which is the fundamental solution of the isotropic Mindlin operator (20), is defined by (see, e.g., [28])

$$L_{ik}^M G_{kj}^M(\mathbf{R}) = -\delta_{ij} \delta(\mathbf{R}), \quad (41)$$

where  $\delta(\cdot)$  is the Dirac delta function.

The two-dimensional Green tensor of the plane strain problem in Mindlin's strain gradient elasticity is given by (see [14, 28, 42])

$$G_{ij}^M(\mathbf{R}) = \frac{1}{8\pi\mu} \left[ (\delta_{ij} \Delta - \partial_i \partial_j) A(\mathbf{R}, \ell_2) + \frac{1-2\nu}{2(1-\nu)} \partial_i \partial_j A(\mathbf{R}, \ell_1) \right] \quad (42)$$

<sup>1</sup> In simplified incompatible strain gradient elasticity, Eq. (38) reads:  $C_{ijkl} \partial_j (L \beta_{kl}^P - \beta_{kl}^{P,0}) = 0$ , leading to the inhomogeneous Helmholtz equation:  $L \beta_{kl}^P = \beta_{kl}^{P,0}$  with  $L = 1 - \ell^2 \Delta$  (see, e.g., [18, 25]).

with the two scalar auxiliary functions

$$A(R, \ell_1) = -\left\{ R^2 \ln R - R^2 + 4\ell_1^2 [\ln R + K_0(R/\ell_1)] \right\}, \quad (43)$$

$$A(R, \ell_2) = -\left\{ R^2 \ln R - R^2 + 4\ell_2^2 [\ln R + K_0(R/\ell_2)] \right\}, \quad (44)$$

where  $i, j = x, y$  and  $\mathbf{R} \in \mathbb{R}^2$ . Here  $K_n$  is the modified Bessel function of the second kind of order  $n$ , and  $\nu$  indicates Poisson's ratio.

For the anti-plane strain problem in Mindlin's strain gradient elasticity, the Green function is defined by (see, e.g., [28])

$$L_{zz}^M G_{zz}^M(\mathbf{R}) = -\delta(\mathbf{R}) \quad (45)$$

with the Mindlin operator of anti-plane strain depending only on the length  $\ell_2$ ,

$$L_{zz}^M = \mu[1 - \ell_2^2 \Delta]. \quad (46)$$

For anti-plane strain, the two-dimensional Mindlin operator simplifies to the two-dimensional Laplace-Helmholtz operator. The two-dimensional Green tensor of the anti-plane strain problem in Mindlin's strain gradient elasticity is given by (see [28])

$$G_{zz}^M(\mathbf{R}) = -\frac{1}{2\pi\mu} [\ln R + K_0(R/\ell_2)], \quad (47)$$

which is non-singular and finite. The gradient of the Green's function (47) reads as

$$\partial_k G_{zz}^M(\mathbf{R}) = -\frac{1}{2\pi\mu} \frac{R_k}{R^2} \left( 1 - \frac{R}{\ell_2} K_1(R/\ell_2) \right), \quad (48)$$

being non-singular, continuous and zero at  $R = 0$ .

#### 2.4.2 Two-dimensional Green's functions of the Helmholtz and bi-Helmholtz operators

The Green's function of the Helmholtz operator (25) is defined by

$$L_j G^{L_j} = \delta(\mathbf{R}), \quad (49)$$

and its solution reads

$$G^{L_j} = \frac{1}{2\pi\ell_j^2} K_0(R/\ell_j). \quad (50)$$

The Green's function of the bi-Helmholtz operator, which is the product of two Helmholtz operators, is defined by

$$L_i L_j G^{L_i L_j} = \delta(\mathbf{R}) \quad (51)$$

and reads (see, e.g., [21])

$$G^{L_i L_j} = \frac{1}{2\pi} \frac{1}{\ell_i^2 - \ell_j^2} [K_0(R/\ell_i) - K_0(R/\ell_j)] \quad (52)$$

for  $i \neq j$ . Of course, it yields

$$G^{L_i L_j} = G^{L_i} * G^{L_j}, \quad (53)$$

where  $*$  denotes the convolution.

## 2.5 Solutions for the displacement vector and the plastic distortion tensor

Using the technique of Green's functions, the solution of Eq. (40) reads for the displacement vector

$$u_i = -\mu \partial_k G_{ij}^M * (\beta_{jk}^{P,0} + \beta_{kj}^{P,0}) - \lambda \partial_j G_{ij}^M * \beta_{kk}^{P,0}. \quad (54)$$

For the plastic distortion, Eq. (38) must be solved. The divergence of Eq. (38) yields

$$2\mu L_4 \partial_k \partial_l \hat{\beta}_{kl}^P + \frac{1}{3}(2\mu + 3\lambda)L_3 \Delta \beta_{ll}^P = 2\mu \partial_k \partial_l \hat{\beta}_{kl}^{P,0} + \frac{1}{3}(2\mu + 3\lambda) \Delta \beta_{ll}^{P,0}. \quad (55)$$

We consider dislocations that incur no volume change (dislocations of glide mode), so that the plastic dilatation must be zero,

$$\beta_{ll}^P = 0, \quad (56)$$

and the classical plastic dilatation must be zero,

$$\beta_{ll}^{P,0} = 0. \quad (57)$$

That means that the plastic dilatation must be zero for dislocations of glide mode. Then, Eq. (55) reduces to

$$L_4 \partial_k \partial_l \hat{\beta}_{kl}^P = \partial_k \partial_l \hat{\beta}_{kl}^{P,0}, \quad (58)$$

and the solution of Eq. (58) can be written as

$$\partial_k \partial_l \hat{\beta}_{kl}^P = G^{L_4} * \partial_k \partial_l \hat{\beta}_{kl}^{P,0}. \quad (59)$$

If we substitute Eq. (59) into Eq. (38), under consideration of Eqs. (56) and (57), we obtain the following solution:

$$\partial_l \hat{\beta}_{il}^P + \partial_l \hat{\beta}_{li}^P = G^{L_2} * (\partial_l \hat{\beta}_{il}^{P,0} + \partial_l \hat{\beta}_{li}^{P,0}) - 2(\ell_2^2 - \ell_4^2) G^{L_2 L_4} * \partial_i \partial_k \partial_l \hat{\beta}_{kl}^{P,0}. \quad (60)$$

Therefore, the solution for the divergence of the deviatoric plastic strain tensor is given by Eq. (60).

## 2.6 Material parameters

It is important to point out that both the elastic constants ( $\mu$ ,  $\lambda$ ) and the gradient elastic constants ( $a_1$ ,  $a_2$ ,  $a_3$ ,  $a_4$ ,  $a_5$ ) are characteristic material parameters which can be computed from interatomic potentials (e.g., [44]) or via ab initio DFT calculations (e.g., [45]). Therefore, the characteristic length scale parameters are also characteristic material parameters given in terms of the elastic constants and gradient elastic constants by Eqs. (21), (22), (26), and (27).

For the numerical analysis of the elastic and plastic fields produced by screw and edge dislocations, we choose aluminum (Al) which is a nearly isotropic material [2]. The Lamé constants, gradient elastic constants, characteristic lengths, equilibrium lattice parameter and Poisson's ratio of aluminum, which have been calculated via ab initio DFT by Shodja et al. [45] and Shodja [46], are given in Table 1. It is interesting to note that the characteristic length  $\ell_2$  is the smallest one of the four characteristic lengths for aluminum given in Table 1. For the numerical analysis of screw and edge dislocations in Sects. 3, 4, and 5, we are using the material parameters given in Table 1.

**Table 1** Lamé constants, gradient elastic constants, characteristic lengths, equilibrium lattice parameter and Poisson's ratio for aluminum (Al) computed via ab initio DFT [45,46]

$\lambda$ (eV/Å <sup>3</sup> )	$\mu$ (eV/Å <sup>3</sup> )	$a_1$ (eV/Å)	$a_2$ (eV/Å)	$a_3$ (eV/Å)	$a_4$ (eV/Å)	$a_5$ (eV/Å)
0.4294	0.1701	-0.0028	1.1564	0.2609	-0.0206	0.7158
$\ell_1$ (Å)	$\ell_2$ (Å)	$\ell_3$ (Å)	$\ell_4$ (Å)	$a$ (Å)	$\nu$	
2.3415	1.6582	2.3299	2.3691	4.05	0.3581	

### 3 Screw dislocation

Consider a screw dislocation at the position  $(x, y) = (0, 0)$  whose Burgers vector  $b_z$  and dislocation line coincide with the  $z$ -axis of a Cartesian coordinate system. The problem of a screw dislocation is of anti-plane strain type.

For a screw dislocation, Eqs. (19), (38), and (40) simplify to

$$L_{zz}^M u_z = \mu L_2 \partial_y \beta_{zy}^P, \quad (61)$$

$$L_2 \beta_{zy}^P = \beta_{zy}^{P,0} \quad (62)$$

and

$$L_{zz}^M u_z = \mu \partial_y \beta_{zy}^{P,0}, \quad (63)$$

respectively.<sup>2</sup>

For the classical plastic distortion of a screw dislocation, we choose the expression given by deWit [6] (see also [36])

$$\beta_{zy}^{P,0} = b_z \delta(y) H(-x) = b_z \delta(y) \int_x^\infty \delta(X) dX, \quad (64)$$

possessing a discontinuity at  $y = 0$  for  $x < 0$ . Here  $H(\cdot)$  is the Heaviside step function. The plastic distortion (64) is caused by a relative slip  $b_z$  on the half-plane ( $y = 0, x < 0$ ) in the  $z$ -direction. The classical plastic distortion (64) is concentrated on the slip plane (the semi-infinite part of the  $xz$ -plane for negative  $x$ ). This causes singularities and discontinuities.

If we substitute Eq. (64) into Eq. (62) and use the Green's function (50), the plastic distortion reads in incompatible strain gradient elasticity of Mindlin type

$$\begin{aligned} \beta_{zy}^P &= G^{L_2} * \beta_{zy}^{P,0} \\ &= \frac{b_z}{2\pi \ell_2^2} \int_x^\infty K_0(\sqrt{X^2 + y^2/\ell_2}) dX, \end{aligned} \quad (65)$$

which is non-singular and finite as observed in Fig. 1. Unlike the classical plastic distortion (64), the plastic distortion (65) is a smooth and continuous function in strain gradient elasticity. In gradient elasticity, the plastic distortion is distributed, and as a result, singularities and discontinuities are avoided (see Fig. 1).

The corresponding dislocation density of a screw dislocation reads as

$$\begin{aligned} \alpha_{zz} &= -\partial_x \beta_{zy}^P \\ &= G^{L_2} * \alpha_{zz}^0 \\ &= \frac{b_z}{2\pi \ell_2^2} K_0(r/\ell_2), \end{aligned} \quad (66)$$

<sup>2</sup> Note that Gutkin and Aifantis [8] solved the homogeneous PDE,  $L_{zz}^M u_z = 0$ , for their "displacement field solution" instead of the inhomogeneous PDE (63) with Eq. (64). Consequently, the "Gutkin-Aifantis solution" for the displacement field given in [8,10] does not satisfy the correct equation (63) at  $y = 0$  (see also the discussion in [20]). The same is true for the displacement component  $u_x$  of an edge dislocation given in [9,10].

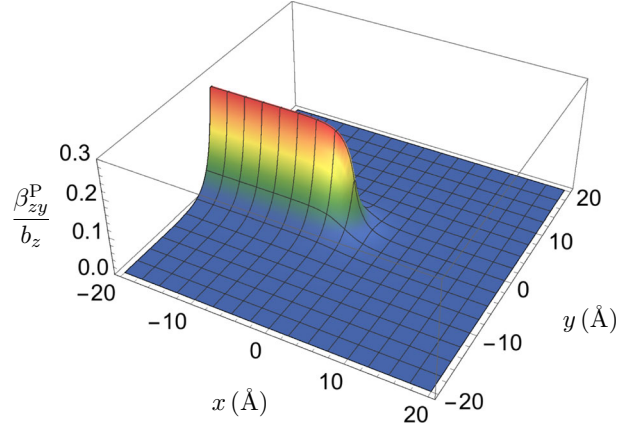


**Fig. 1** Plastic distortion  $\beta_{zy}^P$  of a screw dislocation in incompatible strain gradient elasticity of Mindlin type near the dislocation line

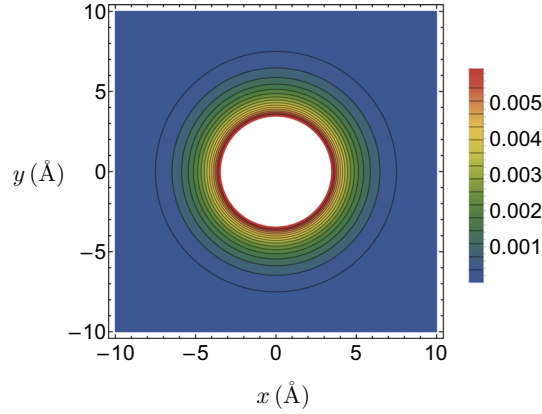


**Fig. 2** Contour plot of the dislocation density of a screw dislocation  $\alpha_{zz}$  (normalized by the Burgers vector  $b_z$ ) in incompatible strain gradient elasticity of Mindlin type

where  $\alpha_{zz}^0 = b_z \delta(x) \delta(y)$  is the classical dislocation density of a screw dislocation and  $r = \sqrt{x^2 + y^2}$ . The dislocation density (66) is plotted in Fig. 2, and it gives the shape and the size of the dislocation core of a screw dislocation. It can be seen that the dislocation core of a screw dislocation possesses a cylindrical symmetry. Such a shape of the dislocation core of a screw dislocation is physical because the Burgers vector, which is in  $z$ -direction, does not break the cylindrical symmetry of the dislocation core of a screw dislocation. Note that the dislocation density (66) possesses a logarithmic singularity at the dislocation line.

Substituting Eq. (64) into Eq. (63) and using the Green's function (47), the displacement field  $u_z$  is calculated as

$$\begin{aligned} u_z &= -\mu \partial_y G_{zz}^M * \beta_{zy}^{P,0} \\ &= -\frac{b_z}{2\pi} \partial_y \int_x^\infty \left[ \ln \sqrt{X^2 + y^2} + K_0 \left( \sqrt{X^2 + y^2} / \ell_2 \right) \right] dX \\ &= \frac{b_z}{2\pi} \left( \arctan \frac{y}{x} + \pi H(-x) \operatorname{sgn}(y) + \partial_y \int_x^\infty K_0 \left( \sqrt{X^2 + y^2} / \ell_2 \right) dX \right), \end{aligned} \quad (67)$$

where the first part in Eq. (67) is the angle  $\varphi$  with range  $(-\pi, \pi]$ , that is  $-\pi < \varphi \leq \pi$ , and discontinuity of  $2\pi$  across the negative  $x$ -axis (see also [6,38])<sup>3</sup>,

$$\varphi = \arctan \frac{y}{x} + \pi H(-x) \operatorname{sgn}(y). \quad (68)$$

<sup>3</sup> Such a form of  $\varphi$  can be used in many modern computer algebra systems by means of particular commands: for instance, `ArcTan[x,y]` in Mathematica and `arctan(y,x)` in Maple.

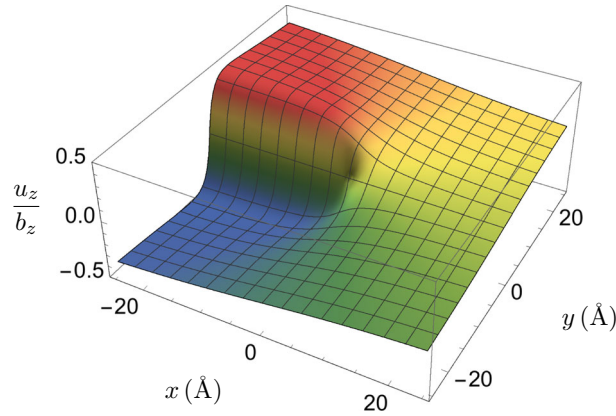


**Fig. 3** Displacement field  $u_z$  of a screw dislocation in incompatible strain gradient elasticity of Mindlin type near the dislocation line

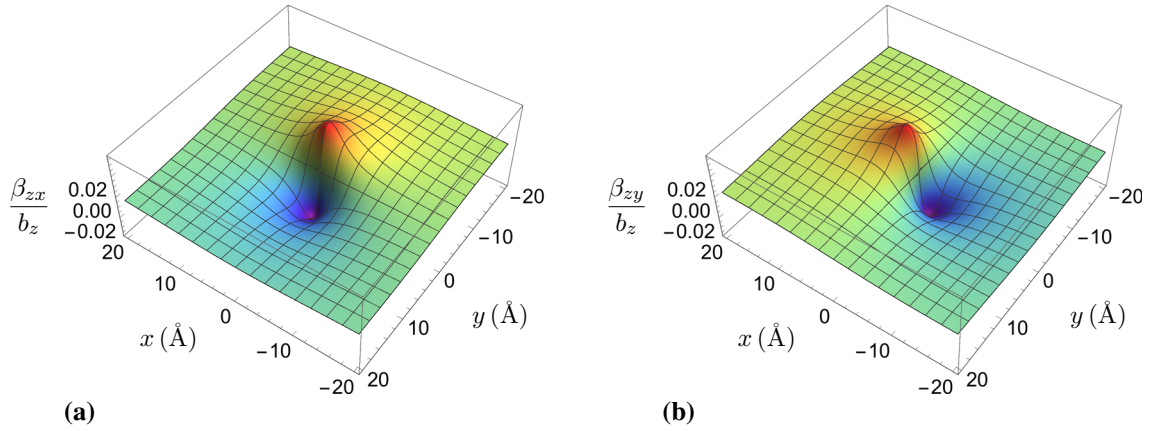


**Fig. 4** Elastic distortion of a screw dislocation in incompatible strain gradient elasticity of Mindlin type near the dislocation line: **a**  $\beta_{zx}$  and **b**  $\beta_{zy}$

The displacement field (67) is plotted in Fig. 3. It is interesting to note that the displacement field (67) is non-singular and has a smooth form due to the superposition of the classical jump discontinuity (first term) and the gradient term (second term). This superposition gives a smoothing of the classical jump discontinuity present in Eq. (68). Therefore, while the displacement field of a screw dislocation in classical dislocation theory possesses a jump discontinuity at the branch cut or dislocation surface ( $y = 0$  and  $x < 0$ ), the jump discontinuity has been smoothed out in strain gradient elasticity. This smoothing of the classical jump discontinuity (68) strongly depends on the value of the length scale parameter  $\ell_2$  and, in particular, on the ratio  $\ell_2/a$  and is a result of the convolution in Eq. (67). In the limit as  $\ell_2 \rightarrow 0$ , we recover the classical discontinuity in the displacement field. Note that the displacement field (67) is in agreement with the expression given in [3].

For a screw dislocation, the non-vanishing components of the elastic distortion are calculated as

$$\beta_{zx} = \mu b_z \partial_y G_{zz}^M = -\frac{b_z}{2\pi} \frac{y}{r^2} \left[ 1 - \frac{r}{\ell_2} K_1(r/\ell_2) \right], \quad (69)$$

$$\beta_{zy} = -\mu b_z \partial_x G_{zz}^M = \frac{b_z}{2\pi} \frac{x}{r^2} \left[ 1 - \frac{r}{\ell_2} K_1(r/\ell_2) \right]. \quad (70)$$

The components of the elastic distortion tensor, Eqs. (69) and (70), are plotted in Fig. 4a, b. It is evident that they are non-singular. The components (69) and (70) of the incompatible elastic distortion tensor satisfy the relation:  $\alpha_{zz} = \partial_x \beta_{zy} - \partial_y \beta_{zx}$ . In the limit  $\ell_2 \rightarrow 0$ , the classical expressions given by deWit [6] are recovered in Eqs. (69) and (70). The non-vanishing components of the Cauchy stress tensor are given by:  $\sigma_{zx} = \mu \beta_{zx}$  and  $\sigma_{zy} = \mu \beta_{zy}$ . All fields (displacement, elastic distortion, plastic distortion, stress, dislocation density) of a screw dislocation depend only on the characteristic length  $\ell_2$ .

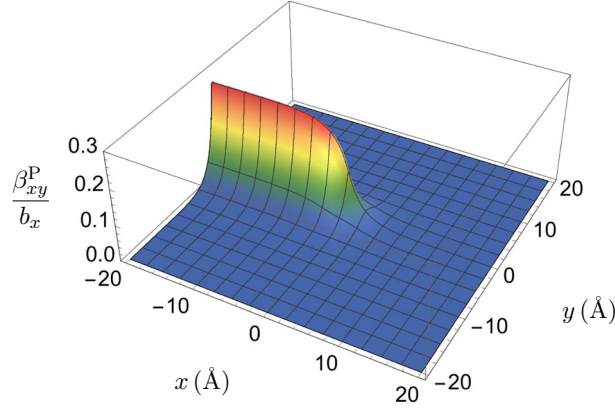


**Fig. 5** Plastic distortion  $\beta_{xy}^P$  of an edge dislocation in incompatible strain gradient elasticity of Mindlin type near the dislocation line

#### 4 Edge dislocation

Consider an edge dislocation at the position  $(x, y) = (0, 0)$  whose Burgers vector  $b_x$  lies in  $x$ -direction and the dislocation line coincides with the  $z$ -axis of a Cartesian coordinate system. The problem of an edge dislocation is of plane strain type.

For the classical plastic distortion of an edge dislocation of glide mode, the expression given by deWit [6] (see also [36]) reads as

$$\beta_{xy}^{P,0} = b_x \delta(y) H(-x) = b_x \delta(y) \int_x^\infty \delta(X) dX. \quad (71)$$

The plastic distortion (71) is caused by a relative slip  $b_x$  on the half-plane ( $y = 0, x < 0$ ) in the  $x$ -direction.

Using Eq. (60), the non-vanishing component of the plastic distortion tensor can be written for an edge dislocation,

$$\begin{aligned} \beta_{xy}^P &= G^{L2} * \beta_{xy}^{P,0} - 2(\ell_2^2 - \ell_4^2) G^{L2L4} * \partial_x^2 \beta_{xy}^{P,0} \\ &= G^{L2} * \beta_{xy}^{P,0} + 2(\ell_2^2 - \ell_4^2) \partial_x G^{L2L4} * \alpha_{xz}^0, \end{aligned} \quad (72)$$

and the corresponding non-vanishing component of the dislocation density tensor reads

$$\begin{aligned} \alpha_{xz} &= -\partial_x \beta_{xy}^P \\ &= G^{L2} * \alpha_{xz}^0 - 2(\ell_2^2 - \ell_4^2) \partial_x^2 G^{L2L4} * \alpha_{xz}^0, \end{aligned} \quad (73)$$

where  $\alpha_{xz}^0 = b_x \delta(x) \delta(y)$  is the classical dislocation density of an edge dislocation.

On the one hand, if we substitute Eq. (71) into Eq. (72) and use the Green's functions (50) and (52), the plastic distortion of the edge dislocation reads in incompatible gradient elasticity of Mindlin type

$$\beta_{xy}^P = \frac{b_x}{2\pi\ell_2^2} \int_x^\infty K_0(\sqrt{X^2 + y^2}/\ell_2) dX - \frac{b_x}{\pi} \frac{x}{r} \left[ \frac{1}{\ell_2} K_1(r/\ell_2) - \frac{1}{\ell_4} K_1(r/\ell_4) \right]. \quad (74)$$

Note that the plastic distortion (74) is non-singular and finite as observed in Fig. 5. It depends on the two characteristic lengths  $\ell_2$  and  $\ell_4$ . Unlike the classical plastic distortion (71), the plastic distortion (74) is a smooth and continuous function in strain gradient elasticity. The first part in Eq. (74) has the same characteristic form as the plastic distortion of a screw dislocation given in Eq. (65).

On the other hand, if we substitute Eq. (71) into Eq. (73) and use the Green's functions (50) and (52), the dislocation density of the edge dislocation reads in incompatible gradient elasticity of Mindlin type

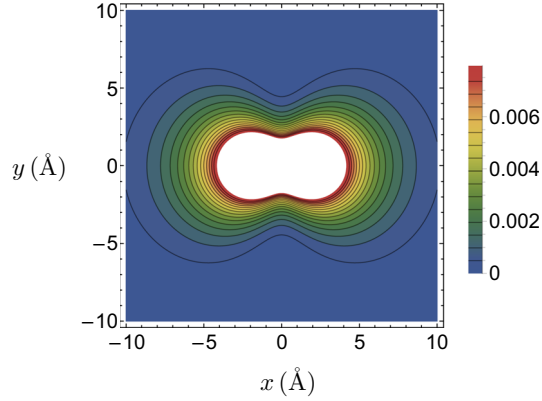


**Fig. 6** Contour plot of the dislocation density of an edge dislocation  $\alpha_{xz}$  (normalized by the Burgers vector  $b_x$ ) in incompatible strain gradient elasticity of Mindlin type

$$\alpha_{xz} = \frac{b_x}{2\pi\ell_2^2} K_0(r/\ell_2) - \frac{b_x}{\pi} \left[ \frac{x^2}{r^2} \left( \frac{1}{\ell_2^2} K_0(r/\ell_2) - \frac{1}{\ell_4^2} K_0(r/\ell_4) \right) + \frac{x^2 - y^2}{r^3} \left( \frac{1}{\ell_2} K_1(r/\ell_2) - \frac{1}{\ell_4} K_1(r/\ell_4) \right) \right]. \quad (75)$$

The dislocation density (75) is plotted in Fig. 6, and it gives the shape and the size of the dislocation core of an edge dislocation. It depends on the two characteristic lengths  $\ell_2$  and  $\ell_4$ . It can be seen that the dislocation core of an edge dislocation does not possess a cylindrical symmetry. Such a shape of the dislocation core of an edge dislocation is physical because the Burgers vector, which is in  $x$ -direction, breaks the cylindrical symmetry of the dislocation core of an edge dislocation toward an asymmetric dislocation core shape. Therefore, an edge dislocation possesses an inherent asymmetry. The first part in Eq. (75) has the same characteristic form as the dislocation density of a screw dislocation given in Eq. (66), whereas the second part in Eq. (75) produces the asymmetric form of the dislocation core of an edge dislocation. For the first time, the asymmetry of the dislocation core inherent in an edge dislocation is modeled in a generalized continuum theory with symmetric stresses revealing the advantage of the considered gradient theory. Until now, the modeling of an asymmetric dislocation core of an edge dislocation was only possible in the framework of the translation gauge theory of dislocations with asymmetric stresses (see [22]).

In order to get the displacement fields of an edge dislocation, the Green tensor (42) is used in Eq. (54) in addition to some mathematical manipulations like Eq. (A.4) and  $\alpha_{xz}^0 = -\partial_x \beta_{zy}^{P,0}$ . In this manner, the displacement fields may be expressed in terms of the auxiliary functions (43) and (44), and the Green's function (47),

$$u_x = -\mu \partial_y G_{zz}^M * \beta_{xy}^{P,0} - \frac{b_x}{4\pi} \left( \partial_y \partial_x A(r, \ell_2) - \frac{1-2\nu}{2(1-\nu)} \partial_y \partial_x A(r, \ell_1) \right), \quad (76)$$

$$u_y = \mu b_x G_{zz}^M - \frac{b_x}{4\pi} \left( \partial_y^2 A(r, \ell_2) - \frac{1-2\nu}{2(1-\nu)} \partial_y^2 A(r, \ell_1) \right). \quad (77)$$

Substituting Eq. (71) into Eq. (76) and using Eqs. (47) and (A.3) in Eqs. (76) and (77), the non-vanishing components of the displacement vector of an edge dislocation read explicitly

$$u_x = \frac{b_x}{2\pi} \left[ \arctan \frac{y}{x} + \pi H(-x) \operatorname{sgn}(y) + \partial_y \int_x^\infty K_0(\sqrt{X^2 + y^2}/\ell_2) dX + \frac{xy}{r^2} \left( 1 - \frac{4\ell_2^2}{r^2} + 2K_2(r/\ell_2) \right) - \frac{1-2\nu}{2(1-\nu)} \frac{xy}{r^2} \left( 1 - \frac{4\ell_1^2}{r^2} + 2K_2(r/\ell_1) \right) \right], \quad (78)$$

$$u_y = -\frac{b_x}{4\pi} \left[ \frac{1-2\nu}{1-\nu} \left\{ \ln r + K_0(r/\ell_1) - \frac{x^2 - y^2}{r^2} \left( 1 - \frac{4\ell_1^2}{r^2} + 2K_2(r/\ell_1) \right) \right\} + \frac{x^2 - y^2}{r^2} \left( 1 - \frac{4\ell_2^2}{r^2} + 2K_2(r/\ell_2) \right) \right]. \quad (79)$$

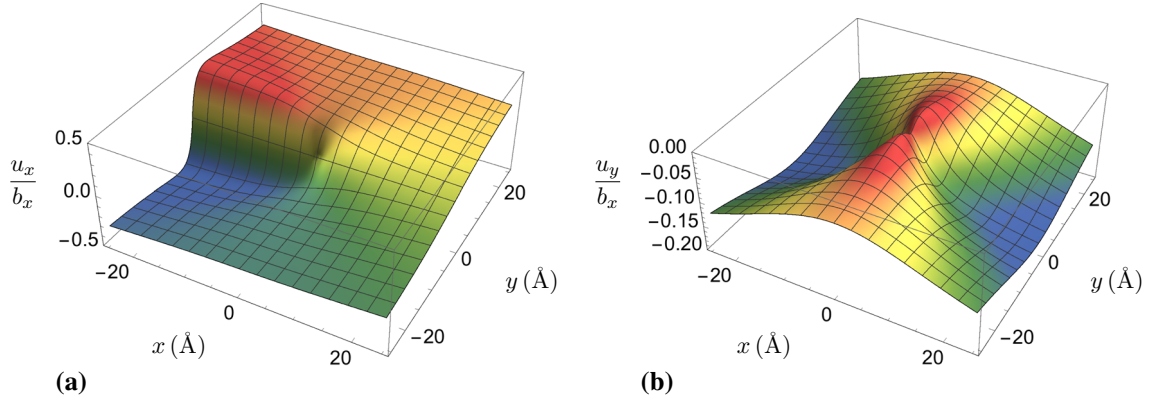


**Fig. 7** Displacement fields of an edge dislocation in incompatible strain gradient elasticity of Mindlin type near the dislocation line: **a**  $u_x$  and **b**  $u_y$

The displacement fields (78) and (79) are plotted in Fig. 7a, b. It is interesting to note that the displacement fields (78) and (79) are non-singular and smooth functions. The first part of Eq. (78) has the same characteristic form as the displacement field of a screw dislocation given in Eq. (67). The displacement fields (78) and (79) depend on the two characteristic lengths  $\ell_1$  and  $\ell_2$ . Note that the displacement fields (78) and (79) agree with the expressions given in [4].

Substituting the plastic distortion (72), the gradient of the displacement fields (76) and (77) into Eq. (3), the incompatible elastic distortion follows as

$$\beta_{xx} = \mu b_x \partial_y G_{zz}^M - \frac{b_x}{4\pi} \left( \partial_y \partial_x^2 A(r, \ell_2) - \frac{1-2\nu}{2(1-\nu)} \partial_y \partial_x^2 A(r, \ell_1) \right), \quad (80)$$

$$\beta_{yy} = \mu b_x \partial_y G_{zz}^M - \frac{b_x}{4\pi} \left( \partial_y^3 A(r, \ell_2) - \frac{1-2\nu}{2(1-\nu)} \partial_y^3 A(r, \ell_1) \right), \quad (81)$$

$$\beta_{xy} = -\mu b_x \partial_x G_{zz}^M - \frac{b_x}{4\pi} \left( \partial_y^2 \partial_x A(r, \ell_2) - \frac{1-2\nu}{2(1-\nu)} \partial_y^2 \partial_x A(r, \ell_1) \right) - 2b_x (\ell_2^2 - \ell_1^2) \partial_x G^{L_2 L_4}, \quad (82)$$

$$\beta_{yx} = \mu b_x \partial_x G_{zz}^M - \frac{b_x}{4\pi} \left( \partial_y^2 \partial_x A(r, \ell_2) - \frac{1-2\nu}{2(1-\nu)} \partial_y^2 \partial_x A(r, \ell_1) \right). \quad (83)$$

Using now Eq. (A.5) for the third-order derivatives, Eq. (48) for the gradient of the Green's function  $G_{zz}^M$  and the Green's function of the bi-Helmholtz operator (52), the non-vanishing components (80)–(83) of the incompatible elastic distortion tensor of an edge dislocation are found to be

$$\begin{aligned} \beta_{xx} = & -\frac{b_x}{4\pi(1-\nu)} \frac{y}{r^2} \left[ (1-2\nu) + \frac{2x^2}{r^2} \right. \\ & - 2(1-\nu) \left\{ \frac{3x^2 - y^2}{r^2} \left( \frac{4\ell_2^2}{r^2} - 2K_2(r/\ell_2) \right) - \frac{x^2 - y^2}{\ell_2 r} K_1(r/\ell_2) \right\} \\ & \left. + (1-2\nu) \left\{ \frac{3x^2 - y^2}{r^2} \left( \frac{4\ell_1^2}{r^2} - 2K_2(r/\ell_1) \right) - \frac{2x^2}{\ell_1 r} K_1(r/\ell_1) \right\} \right], \quad (84) \end{aligned}$$

$$\begin{aligned} \beta_{yy} = & -\frac{b_x}{4\pi(1-\nu)} \frac{y}{r^2} \left[ (1-2\nu) - \frac{2x^2}{r^2} \right. \\ & + 2(1-\nu) \left\{ \frac{3x^2 - y^2}{r^2} \left( \frac{4\ell_2^2}{r^2} - 2K_2(r/\ell_2) \right) - \frac{x^2 - y^2}{\ell_2 r} K_1(r/\ell_2) \right\} \\ & \left. - (1-2\nu) \left\{ \frac{3x^2 - y^2}{r^2} \left( \frac{4\ell_1^2}{r^2} - 2K_2(r/\ell_1) \right) + \frac{2y^2}{\ell_1 r} K_1(r/\ell_1) \right\} \right], \quad (85) \end{aligned}$$

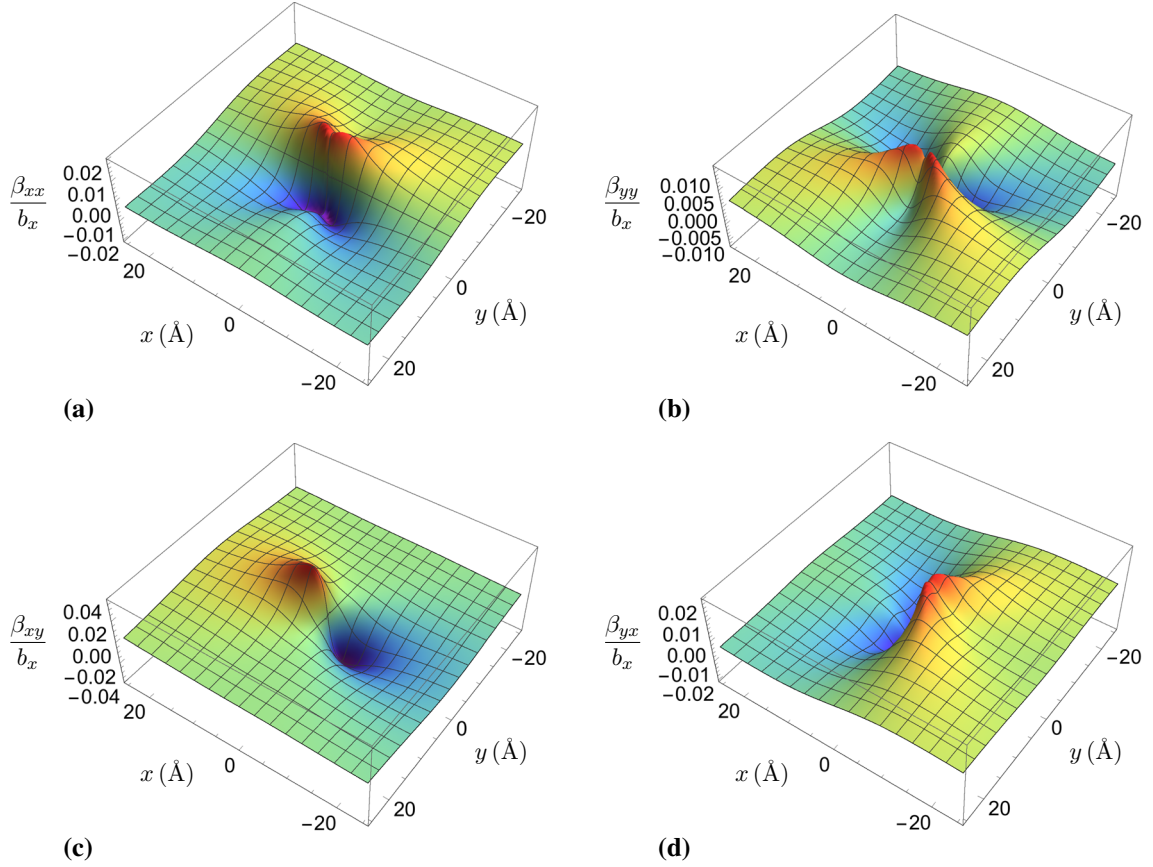


**Fig. 8** Elastic distortion components of an edge dislocation in incompatible strain gradient elasticity of Mindlin type near the dislocation line: **a**  $\beta_{xx}$ , **b**  $\beta_{yy}$ , **c**  $\beta_{xy}$  and **d**  $\beta_{yx}$

$$\begin{aligned} \beta_{xy} = & \frac{b_x}{4\pi(1-\nu)} \frac{x}{r^2} \left[ (3-2\nu) - \frac{2y^2}{r^2} + 4(1-\nu) \left\{ \frac{r}{\ell_2} K_1(r/\ell_2) - \frac{r}{\ell_4} K_1(r/\ell_4) \right\} \right. \\ & - 2(1-\nu) \left\{ \frac{x^2-3y^2}{r^2} \left( \frac{4\ell_2^2}{r^2} - 2K_2(r/\ell_2) \right) + \frac{x^2+3y^2}{\ell_2 r} K_1(r/\ell_2) \right\} \\ & \left. + (1-2\nu) \left\{ \frac{x^2-3y^2}{r^2} \left( \frac{4\ell_1^2}{r^2} - 2K_2(r/\ell_1) \right) + \frac{2y^2}{\ell_1 r} K_1(r/\ell_1) \right\} \right], \end{aligned} \quad (86)$$

$$\begin{aligned} \beta_{yx} = & -\frac{b_x}{4\pi(1-\nu)} \frac{x}{r^2} \left[ (1-2\nu) + \frac{2y^2}{r^2} \right. \\ & + 2(1-\nu) \left\{ \frac{x^2-3y^2}{r^2} \left( \frac{4\ell_2^2}{r^2} - 2K_2(r/\ell_2) \right) - \frac{x^2-y^2}{\ell_2 r} K_1(r/\ell_2) \right\} \\ & \left. - (1-2\nu) \left\{ \frac{x^2-3y^2}{r^2} \left( \frac{4\ell_1^2}{r^2} - 2K_2(r/\ell_1) \right) + \frac{2y^2}{\ell_1 r} K_1(r/\ell_1) \right\} \right]. \end{aligned} \quad (87)$$

The components of the elastic distortion tensor, Eqs. (84)–(87), are plotted in Fig. 8a–d. It can be observed that they are non-singular and zero at the dislocation line. The elastic distortion fields, Eqs. (84)–(87), depend on the three characteristic lengths  $\ell_1$ ,  $\ell_2$ , and  $\ell_4$ . The component  $\beta_{xy}$  is larger than the other three components in the near field (see Fig. 8c). Note that the components (84) and (86) of the incompatible elastic distortion tensor satisfy the relation:  $\alpha_{xz} = \partial_x \beta_{xy} - \partial_y \beta_{xx}$ .

The elastic dilatation, which is the trace of the elastic distortion tensor, reads

$$\beta_{ll} = -\frac{b_x(1-2\nu)}{2\pi(1-\nu)} \frac{y}{r^2} \left[ 1 - \frac{r}{\ell_1} K_1(r/\ell_1) \right]. \quad (88)$$

The elastic rotation, which is the skew-symmetric part of the elastic distortion tensor, reads

$$\omega_{xy} = \frac{b_x}{2\pi} \frac{x}{r^2} \left[ 1 - \frac{r}{\ell_4} K_1(r/\ell_4) \right]. \quad (89)$$

In Eqs. (88) and (89), one can see that in the case of an edge dislocation  $\ell_1$  and  $\ell_4$  are the characteristic lengths for the elastic dilatation and elastic rotation, respectively. The non-vanishing components of the elastic strain tensor are given by:  $e_{xx} = \beta_{xx}$ ,  $e_{yy} = \beta_{yy}$ , and  $e_{xy} = \sigma_{xy}/(2\mu)$ .

Substituting the symmetric part of the elastic distortion tensor given in Eqs. (84)–(87) and the elastic dilatation (88) into the Hooke's law (17) and using the relation  $\lambda = 2\mu\nu/(1 - 2\nu)$ , the non-vanishing components of the Cauchy stress tensor of an edge dislocation are obtained as

$$\begin{aligned} \sigma_{xx} = & -\frac{\mu b_x}{2\pi(1-\nu)} \frac{y}{r^2} \left[ \frac{3x^2 + y^2}{r^2} - \frac{2\nu r}{\ell_1} K_1(r/\ell_1) \right. \\ & - 2(1-\nu) \left\{ \frac{3x^2 - y^2}{r^2} \left( \frac{4\ell_2^2}{r^2} - 2K_2(r/\ell_2) \right) - \frac{x^2 - y^2}{\ell_2 r} K_1(r/\ell_2) \right\} \\ & \left. + (1-2\nu) \left\{ \frac{3x^2 - y^2}{r^2} \left( \frac{4\ell_1^2}{r^2} - 2K_2(r/\ell_1) \right) - \frac{2x^2}{\ell_1 r} K_1(r/\ell_1) \right\} \right], \end{aligned} \quad (90)$$

$$\begin{aligned} \sigma_{yy} = & \frac{\mu b_x}{2\pi(1-\nu)} \frac{y}{r^2} \left[ \frac{x^2 - y^2}{r^2} + \frac{2\nu r}{\ell_1} K_1(r/\ell_1) \right. \\ & - 2(1-\nu) \left\{ \frac{3x^2 - y^2}{r^2} \left( \frac{4\ell_2^2}{r^2} - 2K_2(r/\ell_2) \right) - \frac{x^2 - y^2}{\ell_2 r} K_1(r/\ell_2) \right\} \\ & \left. + (1-2\nu) \left\{ \frac{3x^2 - y^2}{r^2} \left( \frac{4\ell_1^2}{r^2} - 2K_2(r/\ell_1) \right) + \frac{2y^2}{\ell_1 r} K_1(r/\ell_1) \right\} \right], \end{aligned} \quad (91)$$

$$\begin{aligned} \sigma_{xy} = & \frac{\mu b_x}{2\pi(1-\nu)} \frac{x}{r^2} \left[ \frac{x^2 - y^2}{r^2} + 2(1-\nu) \left\{ \frac{r}{\ell_2} K_1(r/\ell_2) - \frac{r}{\ell_4} K_1(r/\ell_4) \right\} \right. \\ & - 2(1-\nu) \left\{ \frac{x^2 - 3y^2}{r^2} \left( \frac{4\ell_2^2}{r^2} - 2K_2(r/\ell_2) \right) + \frac{2y^2}{\ell_2 r} K_1(r/\ell_2) \right\} \\ & \left. + (1-2\nu) \left\{ \frac{x^2 - 3y^2}{r^2} \left( \frac{4\ell_1^2}{r^2} - 2K_2(r/\ell_1) \right) + \frac{2y^2}{\ell_1 r} K_1(r/\ell_1) \right\} \right], \end{aligned} \quad (92)$$

$$\sigma_{zz} = -\frac{\mu\nu b_x}{\pi(1-\nu)} \frac{y}{r^2} \left[ 1 - \frac{r}{\ell_1} K_1(r/\ell_1) \right]. \quad (93)$$

The components of the Cauchy stress tensor, Eqs. (90)–(93), are plotted in Fig. 9a–d. It can be seen that they are non-singular. At the dislocation line, the stress is zero. The stress components, Eqs. (90)–(93), depend on the three characteristic lengths  $\ell_1$ ,  $\ell_2$ , and  $\ell_4$ . The component  $\sigma_{xx}$  is larger than the other three components in the near field (see Fig. 9a). Moreover, the contours of the non-zero components of the Cauchy stress tensor, Eqs. (90)–(93), are given in Fig. 10a–d. Using incompatible strain gradient elasticity of Mindlin type, the contours, as shown in Fig. 10a–d, are the non-singular versions of the classical contours (see, e.g., Hirth and Lothe [12]) in terms of three characteristic lengths. The component  $\sigma_{xx}$  possesses the characteristic butterfly shape (see Fig. 10a). Of course, the non-singular stresses caused by an edge dislocation are more “complex” due to the inherent asymmetry. Moreover, it is important to note that the non-singular stresses of an edge dislocation, Eqs. (90)–(93), are in good agreement with the stress fields of an edge dislocation in Al computed in atomistic simulations by Webb III et al. [48] using the discrete and Hardy expressions for  $\sigma_{ij}$ .

Last but not least, concerning the gradient of the elastic strain tensor and the double stress tensor, it should be noted that some components are non-singular and some other ones are singular, for instance, the gradient of elastic dilatation,  $\partial_i \beta_{ll}$ , appearing in the double stress tensor (18), is still singular.

## 5 Screw and edge dislocations in simplified incompatible strain gradient elasticity

Now, we perform the limit from incompatible strain gradient elasticity of Mindlin type to simplified incompatible strain gradient elasticity (gradient elasticity of Helmholtz type) for the fields of screw and edge dislocations

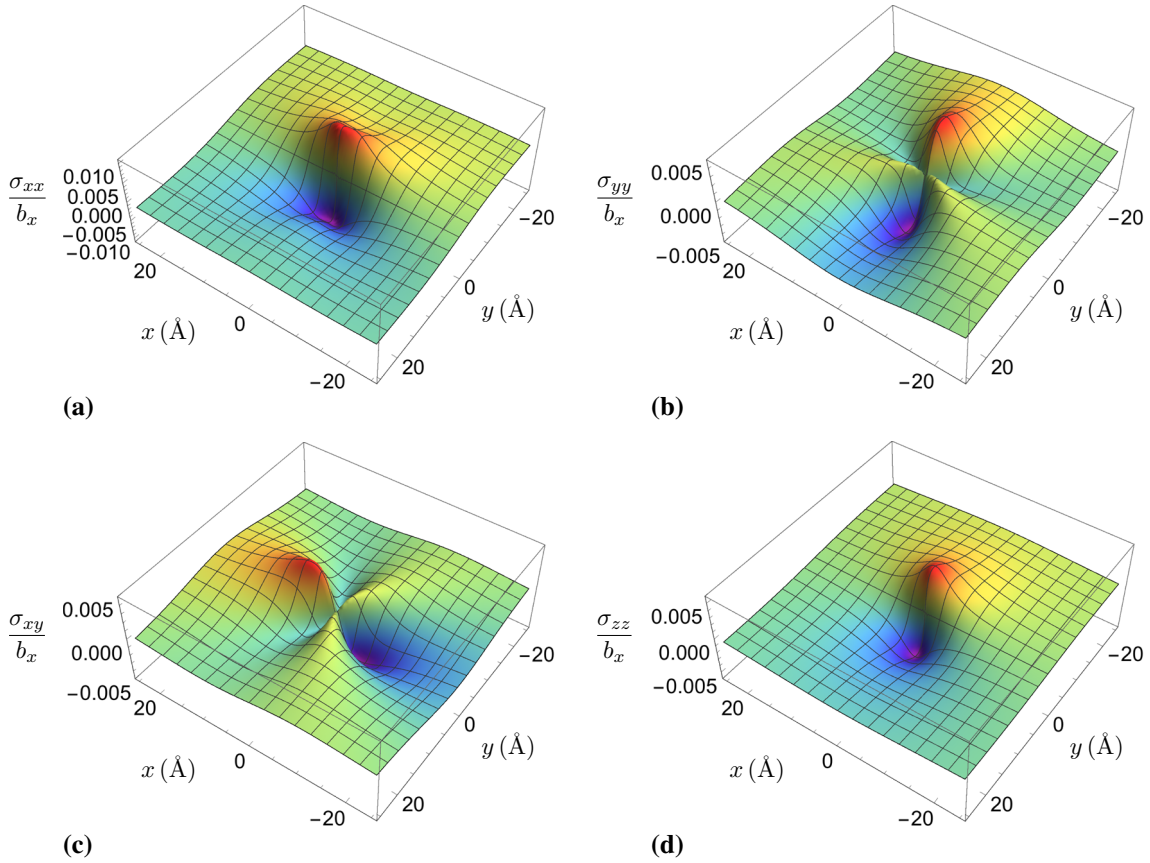


**Fig. 9** Stress components of an edge dislocation in incompatible strain gradient elasticity of Mindlin type near the dislocation line: **a**  $\sigma_{xx}$ , **b**  $\sigma_{yy}$ , **c**  $\sigma_{xy}$ , and **d**  $\sigma_{zz}$

in order to check if the solutions in incompatible strain gradient elasticity of Mindlin type recover the correct ones in simplified incompatible strain gradient elasticity known in the literature. The limit to simplified incompatible strain gradient elasticity is given by [18,28]

$$a_1 = 0, \quad a_2 = \frac{\lambda \ell^2}{2}, \quad a_3 = 0, \quad a_4 = \mu \ell^2, \quad a_5 = 0 \quad (94)$$

and therefore

$$\ell_1 = \ell_2 = \ell_3 = \ell_4 = \ell. \quad (95)$$

For the case of a screw dislocation, the limit reads as  $\ell_2 = \ell$  in Eqs. (65), (66), (67), (69), and (70) leading to known results in the literature (see, e.g., [8,11,18,24,27]). Therefore, the dislocation fields of a screw dislocation in incompatible strain gradient elasticity of Mindlin type agree with the dislocation fields of a screw dislocation in simplified incompatible strain gradient elasticity.

In the limit to simplified incompatible gradient elasticity for an edge dislocation, the plastic distortion (74) simplifies to

$$\beta_{xy}^P = \frac{b_x}{2\pi\ell^2} \int_x^\infty K_0(\sqrt{X^2 + y^2}/\ell) dX, \quad (96)$$

and the dislocation density (75) reduces to

$$\alpha_{xz} = \frac{b_x}{2\pi\ell^2} K_0(r/\ell). \quad (97)$$

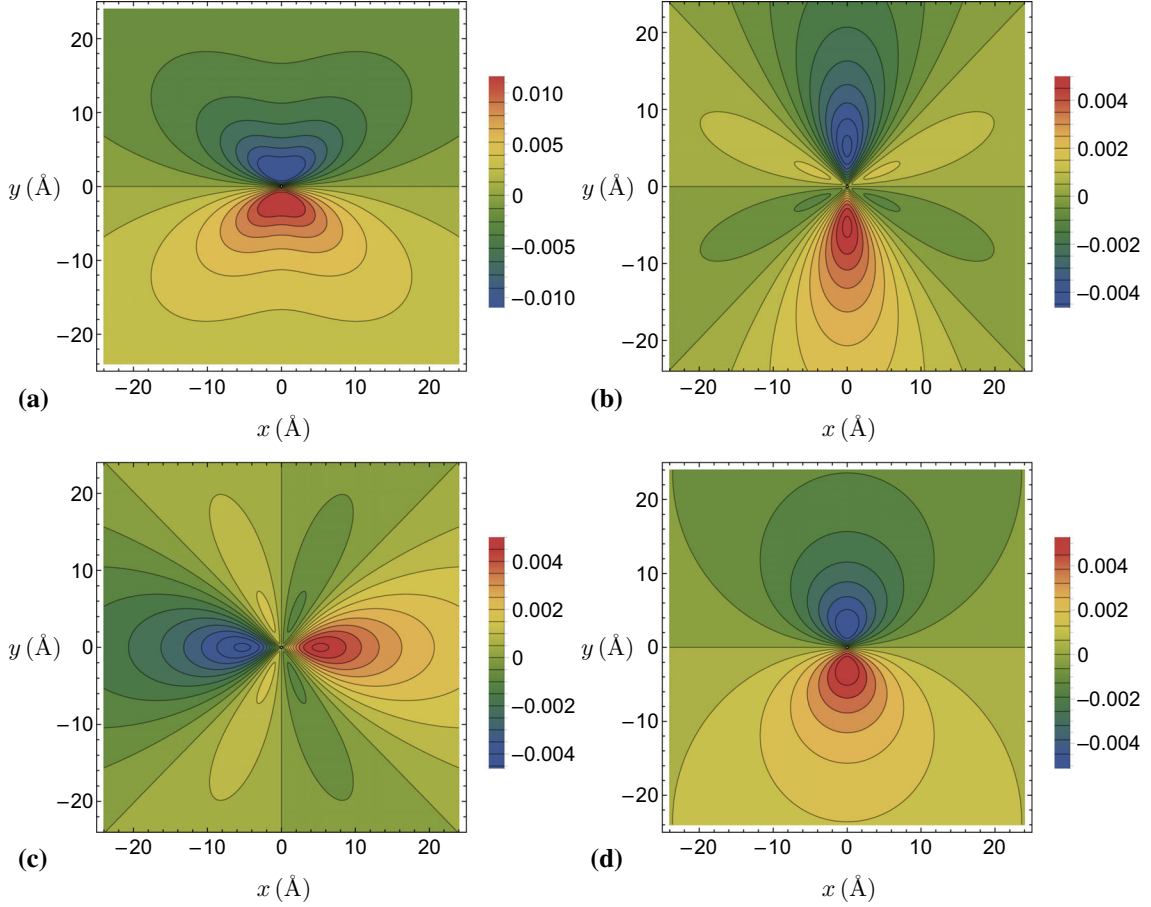


**Fig. 10** Contours of equal stress about an edge dislocation in incompatible strain gradient elasticity of Mindlin type: **a**  $\sigma_{xx}/b_x$ , **b**  $\sigma_{yy}/b_x$ , **c**  $\sigma_{xy}/b_x$ , and **d**  $\sigma_{zz}/b_x$

Of course, Eq. (97) is in agreement with the expression given by Lazar and Maugin [20], Lazar [24,27]. Equation (96) corresponds to the plastic field given in [20,27] with a different branch cut.

The displacement fields (76) and (77) reduce to

$$u_x = \frac{b_x}{4\pi(1-\nu)} \left[ 2(1-\nu) \left( \arctan \frac{y}{x} + \pi H(-x) \operatorname{sgn}(y) + \partial_y \int_x^\infty K_0(\sqrt{X^2 + y^2}/\ell) dX \right) + \frac{xy}{r^2} \left( 1 - \frac{4\ell^2}{r^2} + 2K_2(r/\ell) \right) \right], \quad (98)$$

$$u_y = -\frac{b_x}{4\pi(1-\nu)} \left[ (1-2\nu) \left( \ln r + K_0(r/\ell) \right) + \frac{x^2 - y^2}{2r^2} \left( 1 - \frac{4\ell^2}{r^2} + 2K_2(r/\ell) \right) \right]. \quad (99)$$

Equation (98) is in agreement with the displacement field given in [20,27] up to a different branch cut (see also [11]) and in full agreement with the displacement field given in [4]. Equation (99) agrees with the expression given in [4,9,11,20,27] up to a constant displacement. Note that the component (99) is the non-singular gradient version of the classical displacement field given in [12,41].

Moreover, the incompatible elastic distortion fields (84)–(87) simplify to

$$\beta_{xx} = -\frac{b_x}{4\pi(1-\nu)} \frac{y}{r^2} \left[ (1-2\nu) + \frac{2x^2}{r^2} - \frac{3x^2 - y^2}{r^2} \left( \frac{4\ell^2}{r^2} - 2K_2(r/\ell) \right) - \frac{2(y^2 - \nu r^2)}{\ell r} K_1(r/\ell) \right], \quad (100)$$

$$\beta_{yy} = -\frac{b_x}{4\pi(1-\nu)} \frac{y}{r^2} \left[ (1-2\nu) - \frac{2x^2}{r^2} + \frac{3x^2 - y^2}{r^2} \left( \frac{4\ell^2}{r^2} - 2K_2(r/\ell) \right) - \frac{2(x^2 - \nu r^2)}{\ell r} K_1(r/\ell) \right], \quad (101)$$

$$\beta_{xy} = \frac{b_x}{4\pi(1-\nu)} \frac{x}{r^2} \left[ (3-2\nu) - \frac{2y^2}{r^2} - \frac{x^2 - 3y^2}{r^2} \left( \frac{4\ell^2}{r^2} - 2K_2(r/\ell) \right) - \frac{2(y^2 + (1-\nu)r^2)}{\ell r} K_1(r/\ell) \right], \quad (102)$$

$$\beta_{yx} = -\frac{b_x}{4\pi(1-\nu)} \frac{x}{r^2} \left[ (1-2\nu) + \frac{2y^2}{r^2} + \frac{x^2 - 3y^2}{r^2} \left( \frac{4\ell^2}{r^2} - 2K_2(r/\ell) \right) - \frac{2(x^2 - \nu r^2)}{\ell r} K_1(r/\ell) \right], \quad (103)$$

which agree with the formulas given by Lazar and Maugin [20], Lazar [24, 27]. The comparison of the non-zero components of the elastic distortion tensor of an edge dislocation in strain gradient elasticity of Mindlin type (Eqs. (84)–(87)), simplified strain gradient elasticity (Eqs. (100)–(103)), and classical incompatible elasticity is given in Fig. 11a–d. It is interesting to observe that all four components of the elastic distortion tensor of an edge dislocation using strain gradient elasticity of Mindlin type and simplified strain gradient elasticity are in good agreement, even the “strange” behavior (with two additional zeros) of the near field of the component  $\beta_{yy}$  is reproduced in both gradient theories (see Fig. 11b).

The stress fields (90)–(93) reduce to

$$\sigma_{xx} = -\frac{\mu b_x}{2\pi(1-\nu)} \frac{y}{r^4} \left[ (3x^2 + y^2) - (3x^2 - y^2) \left( \frac{4\ell^2}{r^2} - 2K_2(r/\ell) \right) - \frac{2y^2 r}{\ell} K_1(r/\ell) \right], \quad (104)$$

$$\sigma_{yy} = \frac{\mu b_x}{2\pi(1-\nu)} \frac{y}{r^4} \left[ (x^2 - y^2) - (3x^2 - y^2) \left( \frac{4\ell^2}{r^2} - 2K_2(r/\ell) \right) + \frac{2x^2 r}{\ell} K_1(r/\ell) \right], \quad (105)$$

$$\sigma_{xy} = \frac{\mu b_x}{2\pi(1-\nu)} \frac{x}{r^4} \left[ (x^2 - y^2) - (x^2 - 3y^2) \left( \frac{4\ell^2}{r^2} - 2K_2(r/\ell) \right) - \frac{2y^2 r}{\ell} K_1(r/\ell) \right], \quad (106)$$

$$\sigma_{zz} = -\frac{\mu \nu b_x}{\pi(1-\nu)} \frac{y}{r^2} \left[ 1 - \frac{r}{\ell} K_1(r/\ell) \right], \quad (107)$$

which are in agreement with the formulas given by Gutkin and Aifantis [10], Gutkin [11], Lazar and Maugin [18], and Lazar [27]. The contours of the non-zero components of the stress tensor, Eqs. (104)–(107), are given in Fig. 12a–d. If we compare Figs. 12a–c and 10a–c, it can be seen that the stress components  $\sigma_{xx}$ ,  $\sigma_{yy}$ , and  $\sigma_{xy}$  possess a slightly different shape in the dislocation core region. In the dislocation core region, the stress components in Fig. 10a–c are weaker than the corresponding ones in Fig. 12a–c. Using simplified incompatible strain gradient elasticity, the contours, as shown in Fig. 12a–d, are the non-singular versions of the classical contours (see, e.g., Hirth and Lothe [12]) in terms of only one length scale  $\ell$ . The characteristic butterfly shape of the component  $\sigma_{xx}$  is changing slightly its form in the dislocation core region (see Fig. 12a). If we compare Figs. 10b and 12b for the component  $\sigma_{yy}$ , and Figs. 10c and 12c for the component  $\sigma_{xy}$ , the Cauchy stress components, Eqs. (91) and (92), obtained in incompatible strain gradient elasticity of Mindlin type look more realistic and physical in the dislocation core region than the Cauchy stress components, Eqs. (105) and (106), obtained in simplified incompatible strain gradient elasticity. In particular, the “classical” contours of the stress components  $\sigma_{yy}$  and  $\sigma_{xy}$  at  $|x| = |y|$  of zero stress are slightly modified in the dislocation core region (see Fig. 12b, c).

Last but not least, the limit from simplified incompatible strain gradient elasticity to classical incompatible elasticity is given by  $\ell \rightarrow 0$  leading to the well-known results of screw and edge dislocations given by deWit [6].

## 6 Conclusions

The present paper solves the long-standing problem of dislocations in incompatible isotropic strain gradient elasticity theory of Mindlin type. Exact analytical solutions for the displacement fields, elastic distortions, Cauchy stresses, plastic distortions, and dislocation densities of screw and edge dislocations have been derived. The technique of Green’s functions for PDEs of higher order has been used. For the numerical study of the dislocation fields, elastic constants and strain gradient parameters for Al have been used taken from ab initio

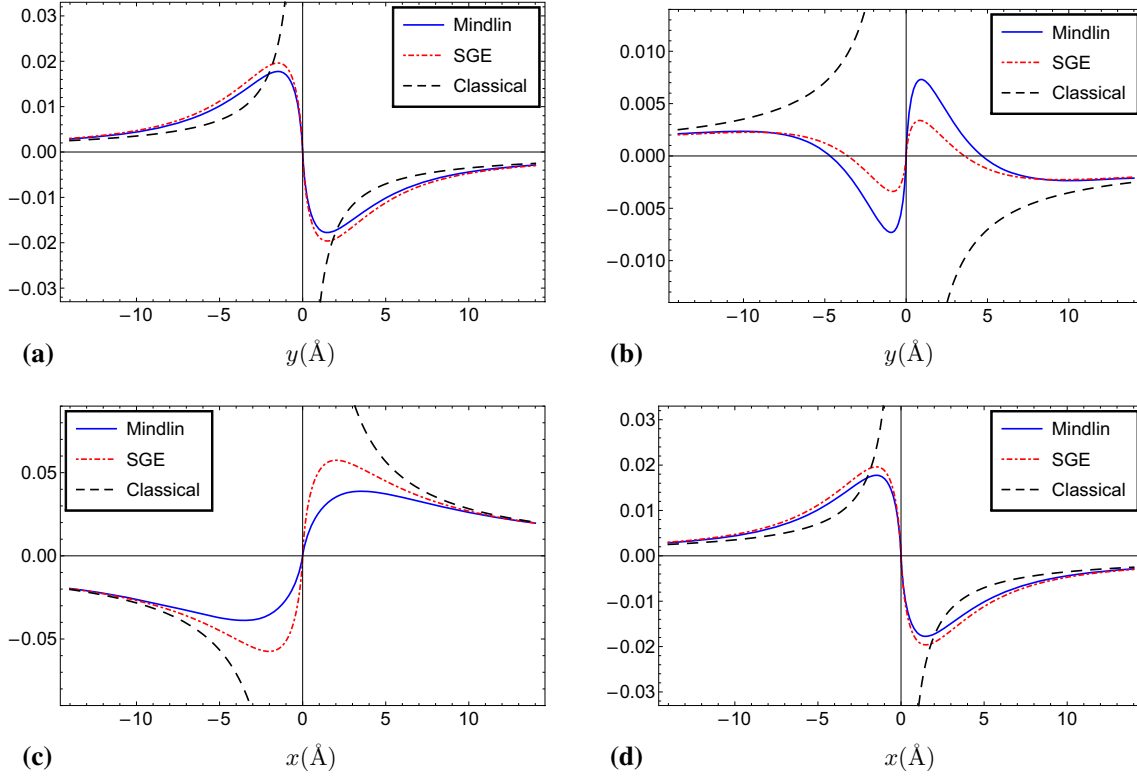


**Fig. 11** Plots of the elastic distortion components of an edge dislocation in incompatible strain gradient elasticity of Mindlin type (Mindlin), simplified incompatible strain gradient elasticity (SGE) for  $\ell = \ell_2$  and classical incompatible elasticity (Classical): **a**  $\beta_{xx}/b_x$ , **b**  $\beta_{yy}/b_x$ , **c**  $\beta_{xy}/b_x$ , and **d**  $\beta_{yx}/b_x$

DFT calculations. As characteristic fact of incompatible gradient elasticity, the analytical solutions for the displacement fields, elastic distortions, stresses, plastic distortions of screw and edge dislocations are non-singular and finite and depend on the characteristic lengths of incompatible isotropic strain gradient elasticity of Mindlin type. The characteristic fields of a screw dislocation depend on one characteristic length  $\ell_2$ , whereas the characteristic fields of an edge dislocation depend on up to three characteristic lengths  $\ell_1$ ,  $\ell_2$ , and  $\ell_4$ . The most important length for the characteristic dislocation profile of the displacement, plastic distortion and dislocation density fields of screw and edge dislocations is the characteristic length  $\ell_2$ . The dependence of the dislocation fields on the characteristic length scale parameters is as follows:

Screw dislocation:

- displacement field:  $u_z = u_z(\mathbf{r}, \ell_2)$
- plastic distortion:  $\beta_{zy}^p = \beta_{zy}^p(\mathbf{r}, \ell_2)$
- dislocation density:  $\alpha_{zz} = \alpha_{zz}(\mathbf{r}, \ell_2)$
- incompatible elastic distortion:  $\beta_{ij} = \beta_{ij}(\mathbf{r}, \ell_2)$
- Cauchy stress:  $\sigma_{ij} = \sigma_{ij}(\mathbf{r}, \ell_2)$

Edge dislocation:

- displacement field:  $u_i = u_i(\mathbf{r}, \ell_1, \ell_2)$
- plastic distortion:  $\beta_{xy}^p = \beta_{xy}^p(\mathbf{r}, \ell_2, \ell_4)$
- dislocation density:  $\alpha_{xz} = \alpha_{xz}(\mathbf{r}, \ell_2, \ell_4)$
- incompatible elastic distortion:  $\beta_{ij} = \beta_{ij}(\mathbf{r}, \ell_1, \ell_2, \ell_4)$
- Cauchy stress:  $\sigma_{ij} = \sigma_{ij}(\mathbf{r}, \ell_1, \ell_2, \ell_4)$ .

The main feature of the obtained solutions of screw and edge dislocations is the absence of any singularity in the displacement, elastic distortion, plastic distortion and stress fields. For a screw dislocation, all the dislocation fields (displacement, elastic distortion, Cauchy stress, plastic distortion, and dislocation density) obtained in incompatible strain gradient elasticity of Mindlin type agree with the corresponding ones in simplified

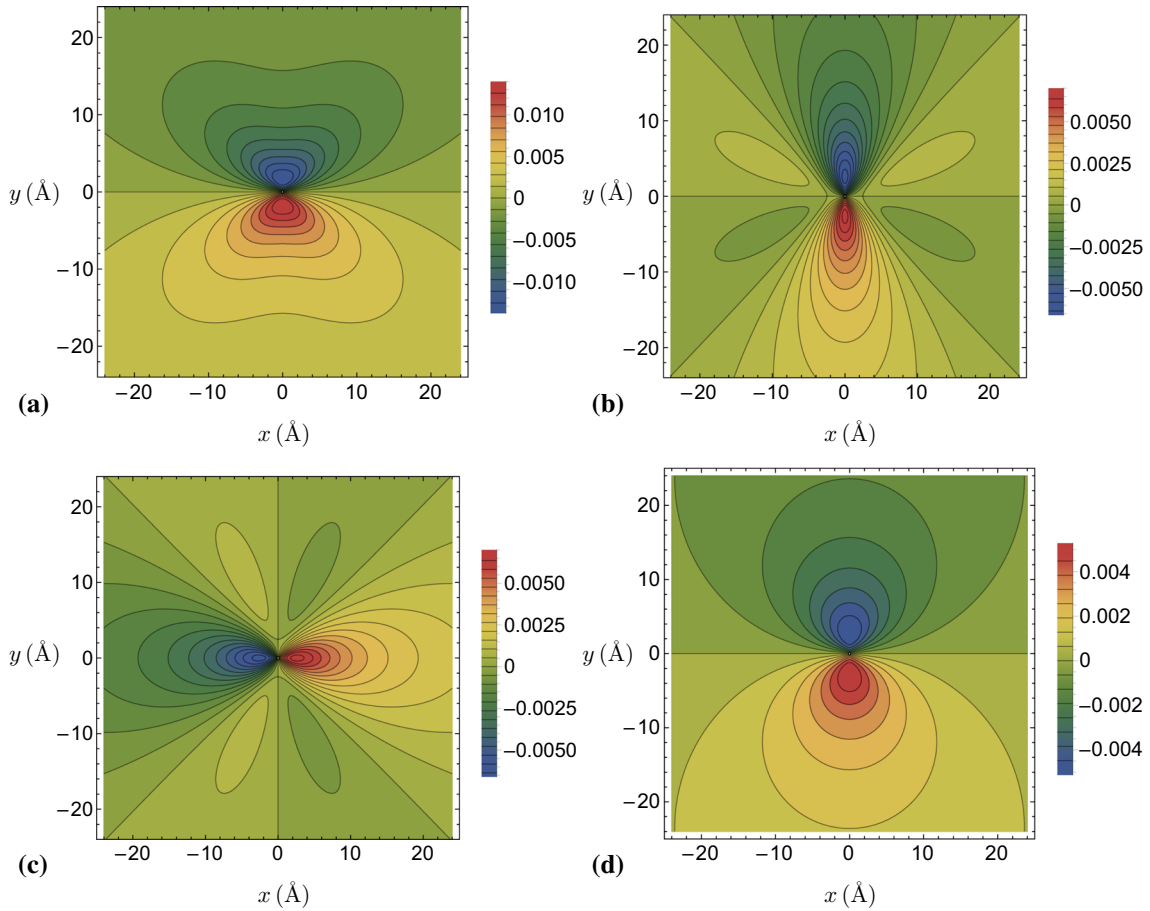


**Fig. 12** Contours of equal stress about an edge dislocation in simplified incompatible strain gradient elasticity for  $\ell = \ell_2$ : **a**  $\sigma_{xx}/b_x$ , **b**  $\sigma_{yy}/b_x$ , **c**  $\sigma_{xy}/b_x$ , and **d**  $\sigma_{zz}/b_x$

incompatible strain gradient elasticity. In the case of an edge dislocation, all the dislocation fields (displacement, elastic distortion, Cauchy stress, plastic distortion, and dislocation density) obtained in incompatible strain gradient elasticity of Mindlin type are different, presenting more features than the corresponding ones in simplified incompatible strain gradient elasticity. For instance, the Cauchy stress of an edge dislocation obtained in incompatible isotropic strain gradient elasticity of Mindlin type looks more physical and more realistic in the dislocation core region than the Cauchy stress obtained in simplified incompatible strain gradient elasticity and is in agreement with the stress around the core of an edge dislocation in Al computed in atomistic simulations. In general, the dislocation core appears naturally in incompatible strain gradient elasticity and is characterized by the dislocation density tensor, which has the physical meaning of a dislocation core tensor. The most exciting fact is that the shape of the dislocation core of an edge dislocation has a more realistic asymmetric form due to its inherent asymmetry in incompatible isotropic strain gradient elasticity of Mindlin type than the dislocation core shape possessing cylindrical symmetry in simplified incompatible strain gradient elasticity. Incompatible isotropic strain gradient elasticity of Mindlin type is a generalized continuum theory with symmetric stress which gives an asymmetric dislocation core for an edge dislocation, and it captures the plastic phenomenon more realistically. Therefore, incompatible strain gradient elasticity of Mindlin type with several characteristic length scale parameters is able to model an edge dislocation more realistically in the dislocation core region than simplified incompatible gradient elasticity with only one length scale. Moreover, incompatible strain gradient elasticity of Mindlin type delivers a better physical based regularization than the regularization with only one regularization parameter in simplified incompatible gradient elasticity. From the dislocation fields obtained in incompatible isotropic strain gradient elasticity theory of Mindlin type, the correct limits for the dislocation fields obtained in simplified incompatible gradient elasticity have been recovered.

**Acknowledgements** Markus Lazar gratefully acknowledges the grant obtained from the Deutsche Forschungsgemeinschaft (grant number LA1974/4-2). The author thanks very much Hossain Shodja for providing and sending the numerical values of the material constants including the gradient elastic constants determined and used in [45]. In addition, the author thanks Ehsan Tavakol for discussing some details of [4]. In particular, the author is grateful to his college Eleni Agiasofitou for many valuable discussions and remarks concerning the physical interpretation of the obtained results and the significance of the presented theory.

**Funding** Open Access funding enabled and organized by Projekt DEAL.

**Open Access** This article is licensed under a Creative Commons Attribution 4.0 International License, which permits use, sharing, adaptation, distribution and reproduction in any medium or format, as long as you give appropriate credit to the original author(s) and the source, provide a link to the Creative Commons licence, and indicate if changes were made. The images or other third party material in this article are included in the article's Creative Commons licence, unless indicated otherwise in a credit line to the material. If material is not included in the article's Creative Commons licence and your intended use is not permitted by statutory regulation or exceeds the permitted use, you will need to obtain permission directly from the copyright holder. To view a copy of this licence, visit <http://creativecommons.org/licenses/by/4.0/>.

## A The auxiliary function $A(R, \ell)$ and its derivatives

We consider the plane strain case with  $\mathbf{R} \in \mathbb{R}^2$ ,  $i, j = x, y$ . For plane strain, the auxiliary function  $A(R, \ell)$  is given by

$$A(R, \ell) = -\left\{R^2 \ln R - R^2 + 4\ell^2 [\ln R + K_0(R/\ell)]\right\}. \quad (\text{A.1})$$

The first-order and second-order derivatives of  $A(R, \ell)$  are given by the following set of equations:

$$\partial_i A(R, \ell) = -\left\{2R_i \ln R - R_i + 4\ell^2 \frac{R_i}{R^2} \left(1 - \frac{R}{\ell} K_1(R/\ell)\right)\right\}, \quad (\text{A.2})$$

$$\partial_j \partial_i A(R, \ell) = -2\delta_{ij} [\ln R + K_0(R/\ell)] + \left(\delta_{ij} - 2\frac{R_i R_j}{R^2}\right) \left(1 - \frac{4\ell^2}{R^2} + 2K_2(R/\ell)\right), \quad (\text{A.3})$$

$$\Delta A(R, \ell) = -4[\ln R + K_0(R/\ell)], \quad (\text{A.4})$$

$$\begin{aligned} \partial_k \partial_j \partial_i A(R, \ell) = & -2 \frac{\delta_{ij} R_k + \delta_{ik} R_j + \delta_{jk} R_i}{R^2} \left(1 - \frac{4\ell^2}{R^2} + 2K_2(R/\ell)\right) \\ & + \frac{4R_i R_j R_k}{R^4} \left(1 - \frac{8\ell^2}{R^2} + 4K_2(R/\ell) + \frac{R}{\ell} K_1(R/\ell)\right) \end{aligned} \quad (\text{A.5})$$

and

$$\partial_k \Delta A(R, \ell) = -4 \frac{R_k}{R^2} \left(1 - \frac{R}{\ell} K_1(R/\ell)\right). \quad (\text{A.6})$$

The expressions (A.1)–(A.6) are non-singular.

## References

1. Admal, N.C., Marian, J., Po, G.: The atomistic representation of first strain-gradient elastic tensors. *J. Mech. Phys. Solids* **99**, 93–115 (2017)
2. Dederichs, P.H., Leibfried, G.: Elastic Green's function for anisotropic cubic crystals. *Phys. Rev.* **188**, 1175–1183 (1969)
3. Delfani, M.R., Tavakol, E.: Uniformly moving screw dislocation in strain gradient elasticity. *Eur. J. Mech. A Solids* **73**, 349–355 (2019)
4. Delfani, M.R., Taaghi, S., Tavakol, E.: Uniform motion of an edge dislocation within Mindlin's first strain gradient elasticity. *Int. J. Mech. Sci.* **179**, 105701 (2020)
5. deWit, R.: Theory of disclinations II. *J. Res. Natl. Bureau Standards* **77A**, 49–100 (1973)
6. deWit, R.: Theory of disclinations IV. *J. Res. Natl. Bureau Standards* **77A**, 607–658 (1973)
7. Eringen, A.C.: *Nonlocal Continuum Field Theories*. Springer, New York (2002)
8. Gutkin, M.Y., Aifantis, E.C.: Screw dislocation in gradient elasticity. *Scripta Mater.* **35**, 1353–1358 (1996)
9. Gutkin, M.Y., Aifantis, E.C.: Edge dislocation in gradient elasticity. *Scripta Mater.* **36**, 129–135 (1997)
10. Gutkin, M.Y., Aifantis, E.C.: Dislocations in gradient elasticity. *Scripta Mater.* **40**, 559–566 (1999)
11. Gutkin, M.Y.: Elastic behaviour of defects in nanomaterials I. *Rev. Adv. Mater. Sci.* **13**, 125–161 (2006)
12. Hirth, J.P., Lothe, J.: *Theory of Dislocations*, 2nd edn. Wiley, New York (1982)
13. Jaunzemis, W.: *Continuum Mechanics*. The Macmillan Company, New York (1967)

14. Karlis, G.F., Charalambopoulos, A., Polyzos, D.: An advanced boundary element method for solving 2D and 3D static problems in Mindlin's strain-gradient theory of elasticity. *Int. J. Numer. Methods Eng.* **83**, 1407–1427 (2010)
15. Kröner, E.: *Kontinuumstheorie der Versetzungen und Eigenspannungen*. Springer, Berlin (1958)
16. Lardner, R.W.: Dislocations in materials with couple stress. *IMA J. Appl. Math.* **7**, 126–137 (1971)
17. Lardner, R.W.: *Mathematical Theory of Dislocations and Fracture*. University of Toronto Press, Toronto (1974)
18. Lazar, M., Maugin, G.A.: Nonsingular stress and strain fields of dislocations and disclinations in first strain gradient elasticity. *Int. J. Eng. Sci.* **43**, 1157–1184 (2005)
19. Lazar, M., Maugin, G.A., Aifantis, E.C.: On dislocations in a special class of generalized elasticity. *Phys. Stat. Sol. (b)* **242**, 2365–2390 (2005)
20. Lazar, M., Maugin, G.A.: Dislocations in gradient elasticity revisited. *Proc. R. Soc. A* **462**, 3465–3480 (2006)
21. Lazar, M., Maugin, G.A., Aifantis, E.C.: On the theory of nonlocal elasticity of bi-Helmholtz type and some applications. *Int. J. Solids Struct.* **43**, 1404–1421 (2006)
22. Lazar, M., Anastassiadis, C.: The gauge theory of dislocations: static solutions of screw and edge dislocations. *Philos. Mag.* **89**, 199–231 (2009)
23. Lazar, M.: Non-singular dislocation loops in gradient elasticity. *Phys. Lett. A* **376**, 1757–1758 (2012)
24. Lazar, M.: The fundamentals of non-singular dislocations in the theory of gradient elasticity: dislocation loops and straight dislocations. *Int. J. Solids Struct.* **50**, 352–362 (2013)
25. Lazar, M.: On gradient field theories: gradient magnetostatics and gradient elasticity. *Philos. Mag.* **94**, 2840–2874 (2014)
26. Lazar, M.: Irreducible decomposition of strain gradient tensor in isotropic strain gradient elasticity. *Zeitschrift für angewandte Mathematik und Mechanik (ZAMM)* **96**, 1291–1305 (2016)
27. Lazar, M.: Non-singular dislocation continuum theories: strain gradient elasticity versus Peierls–Nabarro model. *Philos. Mag.* **97**, 3246–3275 (2017)
28. Lazar, M., Po, G.: On Mindlin's isotropic strain gradient elasticity: Green tensors, regularization, and operator-split. *J. Micromech. Mol. Phys.* **3**(3 & 4), 1840008 (2018)
29. Lazar, M.: A non-singular continuum theory of point defects using gradient elasticity of bi-Helmholtz type. *Philos. Mag.* **99**, 1563–1601 (2019)
30. Lazar, M., Agiasofitou, E., Po, G.: Three-dimensional nonlocal anisotropic elasticity: a generalized continuum theory of Ångström-mechanics. *Acta Mech.* **231**, 743–781 (2020)
31. Li, S., Wang, G.: *Introduction to Micromechanics and Nanomechanics*. World Scientific, Singapore (2008)
32. Mindlin, R.D.: Micro-structure in linear elasticity. *Arch. Ration. Mech. Anal.* **16**, 51–78 (1964)
33. Mindlin, R.D., Eshel, N.N.: On first strain gradient theory in linear elasticity. *Int. J. Solids Struct.* **4**, 109–124 (1968)
34. Mindlin, R.D.: Elasticity, piezoelectricity and crystal lattice dynamics. *J. Elast.* **2**, 217–282 (1972)
35. MODEL (2014), <https://github.com/giacomo-po/MoDELib>
36. Mura, T.: *Micromechanics of Defects in Solids*, 2nd edn. Martinus Nijhoff, Dordrecht (1987)
37. Ortner, N., Wagner, P.: *Fundamental Solutions of Linear Partial Differential Operators*. Springer, Cham (2015)
38. Pellegrini, Y.-P.: Dynamic Peierls–Nabarro equations for elastically isotropic crystals. *Phys. Rev. B* **81**, 024101 (2010)
39. Po, G., Lazar, M., Seif, D., Ghoniem, N.: Singularity-free dislocation dynamics with strain gradient elasticity. *J. Mech. Phys. Solids* **68**, 161–178 (2014)
40. Po, G., Admal, N.C., Lazar, M.: The Green tensor of Mindlin's anisotropic first strain gradient elasticity. *Mater. Theory* **3**, 3 (2019)
41. Read Jr., W.T.: *Dislocations in Crystals*. McGraw-Hill, New York (1953)
42. Rogula, D.: Some basic solutions in strain gradient elasticity theory of an arbitrary order. *Arch. Mech.* **25**, 43–68 (1973)
43. Ru, C.Q., Aifantis, E.C.: A simple approach to solve boundary-value problems in gradient elasticity. *Acta Mech.* **101**, 59–68 (1993)
44. Shodja, H.M., Tehranchi, A.: A formulation for the characteristic lengths of fcc materials in first strain gradient elasticity via Sutton-Chen potential. *Philos. Mag.* **90**, 1893–1913 (2010), Corrigendum, *Philos. Mag.* **92**, 1170–1171 (2012)
45. Shodja, H.M., Zaheri, A., Tehranchi, A.: Ab initio calculations of characteristic lengths of crystalline materials in first strain gradient elasticity. *Mech. Mater.* **61**, 73–78 (2013)
46. Shodja, H.M.: personal communication, October (2015)
47. Toupin, R.A., Grazier, D.C.: Surface effects and initial stress in continuum and lattice models of elastic crystals, in: *Proceedings of the International Conference on Lattice Dynamics, Copenhagen*, Edited by R.F. Wallis, Pergamon Press pp. 597–602 (1964)
48. Webb, E.B., Zimmerman, J.A., Seel, S.C.: Reconsideration of continuum thermomechanical quantities in atomic scale simulations. *Math. Mech. Solids* **13**(3–4), 221–266 (2008)
49. Zauderer, E.: *Partial Differential Equations of Applied Mathematics*. John Wiley & Sons Inc, New York (1983)